



**HAL**  
open science

## Gradual disaggregation of the casein micelle improves its emulsifying capacity and decreases the stability of dairy emulsions

Fanny Lazzaro, Arnaud Saint-Jalmes, Frédéric Violleau, Christelle Lopez, Mireille Gaucher-Delmas, Marie-Noelle Madec, Eric Beaucher, Frederic Gaucheron

### ► To cite this version:

Fanny Lazzaro, Arnaud Saint-Jalmes, Frédéric Violleau, Christelle Lopez, Mireille Gaucher-Delmas, et al.. Gradual disaggregation of the casein micelle improves its emulsifying capacity and decreases the stability of dairy emulsions. *Food Hydrocolloids*, 2017, 63, pp.189-200. 10.1016/j.foodhyd.2016.08.037 . hal-01369072

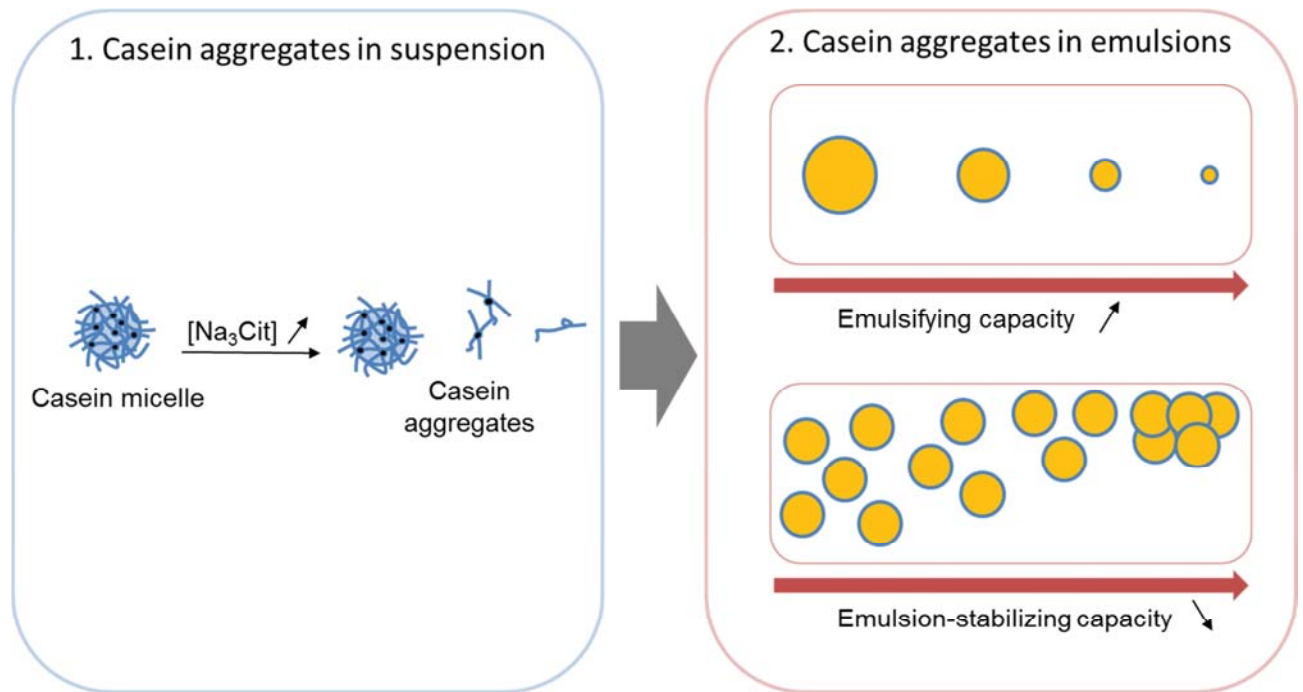
**HAL Id: hal-01369072**

**<https://hal.science/hal-01369072>**

Submitted on 18 Nov 2016

**HAL** is a multi-disciplinary open access archive for the deposit and dissemination of scientific research documents, whether they are published or not. The documents may come from teaching and research institutions in France or abroad, or from public or private research centers.

L'archive ouverte pluridisciplinaire **HAL**, est destinée au dépôt et à la diffusion de documents scientifiques de niveau recherche, publiés ou non, émanant des établissements d'enseignement et de recherche français ou étrangers, des laboratoires publics ou privés.



1 V3 Monday 22<sup>nd</sup> August 2016

2 Gradual disaggregation of the casein micelle improves its emulsifying capacity and  
3 decreases the stability of dairy emulsions

4 Fanny Lazzaro<sup>1,2</sup>, Arnaud Saint-Jalmes<sup>3</sup>, Frédéric Violleau<sup>4</sup>, Christelle Lopez<sup>1</sup>, Mireille  
5 Gaucher-Delmas<sup>5</sup>, Marie-Noëlle Madec<sup>1</sup>, Eric Beaucher<sup>1</sup>, Frédéric Gaucheron<sup>1\*</sup>

6 <sup>1</sup> STLO, Agrocampus Ouest, INRA, 35000, Rennes, France

7 <sup>2</sup> CNIEL, Paris, France

8 <sup>3</sup> Institut de Physique de Rennes, UMR 6251 CNRS-Université Rennes 1, Rennes, France

9 <sup>4</sup> Laboratoire de Chimie Agro-Industrielle (LCA), Université de Toulouse, INRA, INPT, INP-EI  
10 PURPAN, Toulouse, France

11 <sup>5</sup> INP – Ecole d'Ingénieurs de PURPAN, Département Sciences Agronomique &  
12 Agroalimentaires, Université de Toulouse, Toulouse, France

13 \* Corresponding author. STLO, Agrocampus Ouest, INRA, 35000, Rennes, France. Tel.: +33  
14 (0)2 23 48 57 50; fax: +33 (0)2 23 48 53 50. E-mail adress :

15 [frederic.gaucheron@rennes.inra.fr](mailto:frederic.gaucheron@rennes.inra.fr) (F Gaucheron)

## 16 1 Introduction

17 The casein micelle consists of a highly aggregated particle of 150 to 200 nm diameter  
18 constituted of proteins (*i.e.* the four casein molecules  $\alpha_{s1}$ ,  $\alpha_{s2}$ ,  $\beta$ ,  $\kappa$ ), and minerals (mainly  
19 calcium phosphate) that ensure its colloidal stability (Dalgleish & Corredig, 2012; Holt &  
20 Horne, 1996; Holt, Carver, Ecroyd, & Thorn, 2013; Marchin, Putaux, Pignon, & Léonil, 2007;  
21 Schmidt & Payens, 1976; Trejo, Dokland, Jurat-Fuentes, & Harte, 2011; Walstra, 1990). The  
22 casein micelle has a key role in food products, especially dairy products, as it often  
23 contributes to their functional properties (*i.e.* the ability to form and/or stabilize networks such  
24 as gels, foams and emulsions, etc) (Foegeding & Davis, 2011).

25 The colloidal properties of the casein micelle (structure, composition, charge, hydration, etc)  
26 can be modified by controlling environmental factors such as pH, salt and chelating agent  
27 addition, temperature, etc (de Kort, Minor, Snoeren, van Hooijdonk, & van der Linden, 2011;  
28 Gaucheron, 2004; Silva et al., 2013). However, only a few studies have described the link  
29 between the colloidal organization and the functional properties of the modified casein  
30 micelle (Broyard & Gaucheron, 2015). Of all their functional properties, the capacity of the  
31 casein micelle to emulsify and stabilize oil in water emulsions is of great interest for the food  
32 industry, especially for the dairy industry. Indeed, many dairy products are edible emulsions  
33 (*e.g.* cream and ice-cream, infant formulae, etc) (Barbosa-Cánovas, Kokini, Ma, & Ibarz,  
34 1996; Guzey & McClements, 2006).

35 Emulsions consist of mixtures of two immiscible liquids (such as oil and water), one of the  
36 liquids being dispersed as droplets in the other (McClements, 2005). These systems are  
37 thermodynamically unstable. The two phases will separate as a result of creaming,  
38 flocculation (agglomeration) and/or coarsening (fusion by coalescence or Oswald ripening) of  
39 the droplets. It is crucial to control both their formation and their stability during manufacture  
40 and storage to ensure the final quality of food emulsions,.

41 One way to improve the formation and the stability of emulsions is to use emulsifying agents  
42 that adsorb at the oil-water interface and lower its tension. This results in the formation of

43 smaller droplets that are less prone to creaming. The adsorbed layer formed by the  
44 emulsifying agents at the droplet surface can also protect the emulsion against flocculation  
45 and coalescence. Emulsifying agents can be assessed according to two main characteristics:  
46 their ability to facilitate the blending of the emulsion phases (*i.e.* emulsifying capacity) and  
47 their ability to stabilize the emulsion (*i.e.* emulsion-stabilizing capacity). Caseins are known to  
48 adsorb at the interface, either in individual or aggregated form (Dickinson, 1999), and are  
49 therefore able to fulfill the role of emulsifying agent.

50 The emulsifying and stabilizing capacity of caseins is associated with their chemical nature  
51 and conformation at the interface and also depend on their aggregation state. Poorly  
52 aggregated casein systems such as sodium caseinate (30 to 50 nm diameter – formed by  
53 extreme acid demineralization of native casein micelle) (Pitkowski, Durand, & Nicolaï, 2008)  
54 have enhanced emulsifying properties but are less effective for the stabilization of emulsions  
55 than highly aggregated casein micelles (Courthaudon et al., 1999; Mulvihill & Murphy, 1991).  
56 However, little information is available on the emulsifying properties of the intermediate  
57 aggregation states of casein micelles. Ye (2011) contributed to this information by studying  
58 different milk protein concentrates (MPCs) containing both casein and whey proteins as well  
59 as lactose in soya oil-based emulsions. Demineralization of the MPCs was induced by cation  
60 exchange but did not control the diffusible phase.

61 The aim of our study was to investigate the effects of the gradual disaggregation of pure  
62 casein micelles on their colloidal properties and on their emulsifying and stabilizing capacity  
63 in model dairy emulsions. Tri sodium citrate (TSC), a calcium chelating salt, was used to  
64 remove calcium and inorganic phosphate from the casein micelle and to produce four  
65 suspensions of differently demineralized casein aggregates (CAs). Dialysis was performed  
66 on each suspension to control their diffusible phases. The CAs in these suspensions were  
67 characterized physico-chemically and used to form two types of emulsion to study their  
68 emulsifying and emulsion-stabilizing capacity separately. In addition, emulsions containing

69 large droplets were produced to facilitate the creaming during storage and foster the  
70 appearance of flocculation and coalescence.

71

ACCEPTED MANUSCRIPT

## 72 **2 Materials and methods**

### 73 **2.1 Chemicals**

74 All chemicals used for this study, hydrochloric acid (HCl) and tri sodium citrate (TSC) (Carlo  
75 Erba reagent, Val de Reuil, France), sodium azide ( $\text{NaN}_3$ ) (Riedek-de Haën, Seelze,  
76 Germany), sodium hydroxide (NaOH), sodium dodecyl sulfate (SDS), D(+)-saccharose  
77 (saccharose) (VWR international, Leuven, Belgium), calcium chloride dihydrate ( $\text{CaCl}_2 \cdot 2\text{H}_2\text{O}$ )  
78 (Sigma-Aldrich, St. Louis, USA), sodium di-hydrogen phosphate 2-hydrate ( $\text{NaH}_2\text{PO}_4 \cdot 2\text{H}_2\text{O}$ )  
79 (Panreac, Barcelona, Spain), Fast Green FCF (FG) (Sigma-Aldrich, St. Louis, USA) and Nile  
80 Red (NR) (5H-Benzo  $\alpha$ -phenoxazine-5-one, 9-diethylamino, Sigma-Aldrich, St. Louis, USA)  
81 were of analytical grade.

### 82 **2.2 Materials**

83 Purified casein micelles were used to monitor our system. They were supplied by Gillot SAS  
84 (Saint Hilaire de Briouze, France) and obtained by microfiltration (0.1  $\mu\text{m}$  pore size  
85 membrane) of raw skimmed milk followed by diafiltration against milli-Q water and spray  
86 dried according to Pierre, Fauquant, Le Graët, & Maubois (1992) and Schuck et al. (1994) on  
87 Bionov facilities (Rennes, France). The powder comprised 96% (w/w) proteins - especially  
88 caseins (97%) (w/w). Residual whey proteins (3%) (w/w), lactose and diffusible calcium were  
89 present in the powder.

90 Anhydrous milkfat (AMF, melting point 32°C) was supplied by Corman (Limbourg, Belgium).

### 91 **2.3 Preparation of different CA suspensions**

92 Casein micelle powder was suspended in milli-Q water at a concentration of 28 g  $\text{kg}^{-1}$  and  
93  $\text{NaN}_3$  (1.6 g  $\text{kg}^{-1}$ ) was added for conservation (Fig. 1A). To ensure good resuspension of the  
94 powder, the suspension was stirred at 900 rpm for 6 h at 40°C in a water bath and then for  
95 16 hours at room temperature. The rehydration of the casein micelle powder was checked by  
96 laser light diffraction as defined by Schuck, Dolivet, & Jeantet (2012). The results expressed  
97 in volume showed that more than 90 % of the particles were of size of casein micelles (150

98 nm diameter). This suspension was used to prepare four CA suspensions (S1, S2, S3 and  
99 S4). In S2, S3 and S4 varying amounts of a stock solution of TSC ( $0.85 \text{ mol kg}^{-1}$  in milli-Q  
100 water, pH 7.0) were added to reach final concentrations of 4, 13 and  $34 \text{ mmol kg}^{-1}$ ,  
101 respectively. S1 was kept as a control suspension (without addition of TSC). These  
102 suspensions were stirred for 30 min and then diluted with milli-Q water to reach an  
103 intermediate casein concentration of  $25 \text{ g kg}^{-1}$ . The pH was then adjusted to 7.0 with HCl 1M.  
104 S1, S2, S3 and S4 were left overnight at room temperature and the pH of each was  
105 readjusted if necessary.

106 S1, S2, S3 and S4 were then dialyzed against an aqueous solution saturated in calcium and  
107 phosphate ( $5 \text{ mmol kg}^{-1} \text{ NaH}_2\text{PO}_4 \cdot 2\text{H}_2\text{O}$  and  $5 \text{ mmol kg}^{-1}$  of  $\text{CaCl}_2 \cdot 2\text{H}_2\text{O}$ , pH was adjusted to  
108 7.0 using 1 M NaOH). The aim of the dialysis was to remove the added citrate and the ions  
109 solubilized from the casein micelle. This provided an identical ionic environment for all the  
110 CAs in the four different suspensions. Using a solution saturated in calcium and phosphate  
111 also provided the advantage of limiting any further demineralization that might have been  
112 induced by classical dialysis against pure water. This was performed in two steps: first the  
113 suspensions were individually dialyzed (in separate baths) for 27.5 h at room temperature  
114 against a total volume of 44 times each suspension volume, and the baths were changed  
115 four times. The second step was combined dialysis (in the same bath) of the four CA  
116 suspensions for 15 h at room temperature against a volume 11 times the total suspension  
117 volume. The molecular weight cut-off of the dialysis membrane was between 12 and 14 kDa  
118 (Spectra/Por, Rancho Dominguez, Canada). The last dialysis bath was then filtered on a  
119  $2.5 \mu\text{m}$  filter paper and used to dilute the suspensions to reach a final casein concentration of  
120  $19.7 \pm 0.6 \text{ g kg}^{-1}$ . The final pH was  $6.98 \pm 0.04$ . The dialyzed CA suspensions, named S1<sub>d</sub>,  
121 S2<sub>d</sub>, S3<sub>d</sub> and S4<sub>d</sub>, were prepared in duplicate.

#### 122 **2.4 Recovery of the diffusible phases of the CA suspensions**

123 The diffusible phases of each CA suspension were obtained by ultrafiltration for 30 min at  
124  $20^\circ\text{C}$  on Vivaspin 20 concentrators (molecular weight cut-off  $10 \text{ kg mol}^{-1}$ , Vivascience,



125 Palaiseau, France). They were used for the determination of diffusible cation and anion  
126 concentrations in the CA suspensions, as well as for the dilution of the CA suspensions and  
127 the emulsions for determination of the zeta potentials and sizes.

## 128 **2.5 Preparation of the two types of emulsion**

129 Two types of emulsion ( $E^{ec}$  for “emulsifying capacity” and  $E^{st}$  for “stability”) were prepared  
130 with each of the four CA suspensions in order to evaluate the emulsifying and emulsion-  
131 stabilizing capacity of the CAs (Fig. 1B).

132 Emulsions  $E^{ec}$  were prepared with the CA suspensions diluted at a protein concentration of  
133  $1.2 \text{ g kg}^{-1}$  with milli-Q water and then added to the  $60^\circ\text{C}$  melt ed AMF at a 30:70 (v/v) ratio.  
134 The mixture was emulsified at  $50^\circ\text{C}$  in a water bath using a Polytron PT 3100 (Kinematica  
135 AG, Littau, Switzerland) at 29,000 rpm for 5 min. Working at a limited protein concentration  
136 ( $1.20 \text{ g/kg}$  compared to our emulsification system) highlighted the differences between the  
137 CAs by producing emulsions with different droplet sizes.

138  $E^{st}$  emulsions were prepared following the same procedure except that the CA suspensions  
139 were kept at a protein concentration of about  $20 \text{ g kg}^{-1}$ . In this case, the choice of an excess  
140 protein concentration produced emulsions with similar droplet sizes, necessary for the study  
141 of the stabilizing capacity of the CAs.  $E^{st}$  emulsions were divided into several samples and  
142 stored in transparent, cylindrical, hermetically sealed tubes at  $50^\circ\text{C}$  for 3 weeks. The  
143 temperature of  $50^\circ\text{C}$  was chosen in order to prevent the formation of fat crystals in the  
144 emulsion that could affect their physical stability (Lopez, Bourgaux, Lesieur, & Ollivon, 2007).  
145 Each week, one sample was analyzed by laser light diffraction, electrophoretic light  
146 scattering, multiple light scattering and confocal microscopy to follow the evolution of the  
147 emulsion. Two replicate emulsions were made for each type of emulsion.

## 148 **2.6 Analysis**

### 149 **2.6.1 Mineral composition and distribution**

150 Total cations (calcium, magnesium, sodium and potassium) and diffusible cations and anions  
151 (inorganic phosphate, citrate and chloride) were determined in the CA suspensions and in  
152 their diffusible phases, respectively. Total anions were determined in the diffusible phases  
153 CA suspensions previously acidified at pH 4.6 with a 10% (v/v) acetic acid solution. Cation  
154 concentrations were measured by atomic absorption spectrometry (Varian 220FS  
155 spectrometer, Les Ulis, France) as described by Brulé, Maubois & Fauquant (1974). Anion  
156 concentrations were determined by ion chromatography (Dionex ICS 3000, Dionex, Voisin le-  
157 Bretonneux, France) as described by Gaucheron, Le Graët, Piot & Boyaval (1996). Colloidal  
158 concentrations were deduced by subtracting diffusible from total ion concentrations. The  
159 calcium demineralization rates corresponded to the percentage of solubilized calcium  
160 compared to total calcium initially present in the suspensions prior to dialysis.

### 161 **2.6.2 Protein content**

162 Protein content was determined in the CA suspensions and in their respective  
163 ultracentrifuged supernatants to deduce the non-sedimentable casein concentrations. The  
164 Kjeldahl method (IDF standard 20-1,2014) was used to determine the total nitrogen  
165 concentration in the samples, and a conversion factor of 6.38 was used to convert nitrogen to  
166 protein concentration. Measurements were performed in duplicate.

### 167 **2.6.3 Pellet hydration and sedimentable protein concentrations**

168 Twenty grams of CA suspension were ultracentrifuged at 20°C for 1 h at 100,000 *g* (Sorvall  
169 Discovery 90 SE, Hitachi, Courtaboeuf, France) and the ultracentrifuged pellets were  
170 recovered. Hydration was deduced according to the weight loss after drying the  
171 ultracentrifuged pellets of each sample mixed with Fontainebleau sand in an oven at 105°C  
172 for 8 h (FIL-IDF Standard 26A, 1993).

173 Sedimentable protein concentrations were deduced from the proportion of pellets and  
174 hydration data by considering that ultracentrifuged pellets consisted mainly of proteins and  
175 water (mineral weights were disregarded). Measurements were performed in duplicate.

#### 176 **2.6.4 CA sizes and proportions in the CA suspensions (AsFIFFF)**

177 The molecular weights (MW) and hydrodynamic radii ( $R_h$ ) of the CAs were determined in  
178 suspensions S1<sub>d</sub>, S4<sub>d</sub> (extreme points), and S2<sub>d</sub> (intermediate point) using asymmetrical flow  
179 field-flow fractionation (AsFIFFF) coupled to multi angle laser light scattering (MALLS) as  
180 described in Guyomarc'h, Violleau, Surel & Famelart (2010) with slight modifications. A  
181 solution saturated in calcium and phosphate (similar to the solution used for the dialysis step)  
182 was filtered through 0.1  $\mu\text{m}$  filter paper. This filtered solution was used as the eluent for the  
183 AsFIFFF separation, and for the ten-fold dilution of the samples.

184 During the AsFIFFF run, the laminar flow was fixed at 1  $\text{mL min}^{-1}$  and only the cross flow  
185 varied. The first focusing-injection step (10 min) consisted of setting up the cross flow at 1.5  
186  $\text{mL min}^{-1}$  for 1 minute. Then 30  $\mu\text{L}$  of sample were injected while the cross flow was  
187 maintained at 1.5  $\text{mL min}^{-1}$  for 9 min. This allowed the analytes to diffuse away from the  
188 membrane according to their  $R_h$ . The elution step then started with a 5 min plateau at a cross  
189 flow rate of 1  $\text{mL min}^{-1}$  followed by a linear decrease of 5 min to reach 0.15  $\text{mL min}^{-1}$  for 25  
190 min. The cross flow was finally stopped to eliminate all the particles that might have  
191 remained in the AsFIFFF channel.

192 Under our operating conditions, the AsFIFFF worked in normal mode, which means that  
193 larger particles were retained in the channel for longer times than smaller ones, providing  
194 that all particles had similar density.

195 The AsFIFFF was connected to an 18 angle DAWN-DSP MALLS detector (Wyatt  
196 Technology, Santa Barbara, CA, USA) ( $\lambda = 633 \text{ nm}$ ), an Optilab Rex Refractometer (Wyatt  
197 Technology, Santa Barbara, CA, USA) ( $\lambda = 685 \text{ nm}$ ), and an Agilent 1100 UV detector ( $\lambda =$   
198 280 nm). The UV signal was used as the source data for measurement of protein

199 concentrations and a calculated extinction coefficient of  $9.009 \text{ L g}^{-1} \text{ cm}^{-1}$  was determined and  
200 used (bovine serum albumin at 280 nm in the eluent). Astra software version 6.0 was used to  
201 analyze the UV and Rayleigh ratio data and determine the MW and  $R_h$  values. In this study, it  
202 was assumed that the different CAs were spherical and homogenous in composition.  $R_h$   
203 were determined between 20 and 28 min (population A) *via* Berry formalism of a Debye plot.  
204  $R_h$  cannot be calculated directly between 14 to 20 min (populations B and C) because of the  
205 low Rayleigh ratio signal in this time range. For suspensions  $S1_d$  and  $S2_d$ , the  $R_h$  values  
206 between 20 and 24 min were therefore fitted with a first order exponential model that was  
207 extrapolated between 14 and 20 min (populations B and C). This treatment was not possible  
208 on  $S4_d$  because of the low Rayleigh ratio signal, and the values of  $R_h$  determined for  $S4_d$   
209 calculated between 20 and 28 min were not accurate enough for their extrapolation (see  
210 section 3.1.2).

211 Similar tests were performed to determine MW values, with slight modifications. The MW  
212 values of  $S1_d$  and  $S2_d$  were fitted with exponential models of first order between 18 to 20 min  
213 and the models were extrapolated between 14 to 18 min. In contrast to  $R_h$ , the  $S4_d$  Rayleigh  
214 ratio was high enough to determine MW. For this suspension, the MW values were fitted  
215 between 15.5 and 16.5 min (population B) and the model was extrapolated between 14 and  
216 15.5 min (population C).

### 217 **2.6.5 Zeta potential (3)**

218 The electrophoretic mobility of CAs (in CA suspensions) and milkfat droplets (in emulsions)  
219 were measured by electrophoretic light scattering using a Zetasizer 3000 HS (Malvern  
220 Instruments, Worcestershire, UK). CA suspensions and emulsions were diluted in their  
221 corresponding diffusible phases. Diluted CA suspensions were filtered through a  $0.45 \mu\text{m}$   
222 pore size membrane to eliminate possible dust particles prior to analysis.

223 Henry's equation:

$$224 \quad \zeta = ( 3 \eta \mu / 2 \varepsilon f(Ka) ) \quad (1)$$

225 where  $\eta$  is the viscosity and  $\epsilon$  the dielectric constant of the solution, was applied to determine  
226 the apparent zeta potential ( $\zeta$ ) of the particles from their electrophoretic mobility  $\mu$ .  $F(Ka) =$   
227 1.5 was used according to the Smoluchowski approximation. The measurements for the CA  
228 suspensions were performed at 20°C and the viscosity and the dielectric constant of the  
229 dissociating medium (water) were 1.00 cp and 80.4, respectively. Measurements for the  
230 emulsions were performed at 50°C with a viscosity of 0.55 cp and a dielectric constant of  
231 70.2. Measurements were performed in triplicate.

### 232 **2.6.6 Droplet size distribution in emulsions**

233 The milkfat droplet size distributions were determined by laser light diffraction immediately  
234 after the preparation of the emulsions and after 7, 14 and 21 days of storage at 50°C, using a  
235 Mastersizer 2000 (Malvern Instruments, Worcestershire, UK) equipped with a He/Ne laser ( $\lambda$   
236 = 633 nm) and an electroluminescent diode ( $\lambda = 466$  nm). The refractive indices were set at  
237 1.46 (at 466 nm) and 1.458 (at 633 nm) for milkfat and 1.33 for water. Before measurements,  
238 samples were dispersed in milli-Q water as was, or were previously diluted ten times in a  
239 solution of 1% (w/w) SDS to separate aggregated milkfat droplets and estimate the extent of  
240 droplet flocculation. All distributions and/or their corresponding mode values (*i.e.* the maxima  
241 of the size distribution) were used to compare the emulsions. Specific surface areas (area  
242 per unit mass) were used for the determination of the protein surface concentrations.  
243 Measurements were performed in triplicate.

### 244 **2.6.7 Confocal microscopy of the emulsions**

245 The microscopy observations were carried out with a Nikon Eclipse-TE2000-C1si confocal  
246 microscope (Nikon, Champigny sur Marne, France) equipped with argon and He-Ne lasers  
247 operating at 488 and 543 nm excitation wavelengths, respectively (emissions were detected  
248 between 500 and 530 nm and between 565 and 615 nm, respectively). One milliliter of  
249 emulsion was stained using 100  $\mu$ L of a milkfat soluble Nile Red fluorescent dye solution  
250 (0.1% w/w in propane diol) and 50  $\mu$ L of a Fast green FCF solution (1% w/w in water) to stain  
251 the proteins. The samples were left for 15 min at 50°C prior to observation. Microscopy

252 observations were performed at 50°C using a thermal PE100-NI System plate warmer  
253 (Linkam Scientific Instruments Ltd., Tadworth Surrey, England). Images were collected with  
254 an oil immersion objective with a magnification of x 60. Characteristic images were selected  
255 from the 9 images taken for each sample.

### 256 **2.6.8 Interfacial tension and dilatational rheology**

257 An oscillatory drop tensiometer (Tracker, Teclis, France) was used to measure the interfacial  
258 tension ( $\gamma$ ) and the interfacial dilatational moduli ( $E^*$ ,  $E'$  and  $E''$ ) at the milkfat/CA suspension  
259 interfaces, at 50°C. The CA suspensions and the last dialysis bath (control) were used to  
260 form a pendant drop of 10  $\mu$ L at the tip of a syringe that was suspended in an 8 mL cuvette  
261 containing melted milkfat (50°C). Two opposite forces, gravity and the force related to  $\gamma$ ,  
262 were exerted on the drop to induce its shape. Analysis of the shape of the drop 5 min after its  
263 formation (equilibrium state) made it possible to calculate the  $\gamma$  value by solving the Laplace  
264 equation (Ravera, Loglio, & Kovalchuk, 2010).

265 Dilatational rheology was performed on our system by applying the conditions used by Silva,  
266 Saint-Jalmes, de Carvalho, & Gaucheron (2014) with slight modifications. Briefly, a  
267 sinusoidal oscillation of the drop volume of 10% at a frequency of 0.2 Hz was applied to a  
268 2 min old 10 $\mu$ L CA suspension drop in the melted milkfat at 50°C. The volume variation  
269 engendered a controlled oscillatory compression/dilation of the droplet interfacial area  $A$  and  
270 resulted in the surface tension oscillation as a function of time  $\gamma(t)$ . Monitoring of  $\gamma(t)$  and  
271 determination of its phase shift ( $\phi$ ) compared to  $A(t)$  made it possible to calculate the  
272 complex ( $E^*$ ), elastic ( $E'$ ) and viscous ( $E''$ ) moduli of the adsorbed interfacial layer. Purely  
273 elastic and solid-like interfacial layers had  $E' \gg E''$  and  $\phi$  tended to 0, whereas viscous and  
274 fluid-like interfacial layers had  $E'' > E'$  and a large  $\phi$ .

### 275 **2.6.9 Creaming stability ratio**

276 A transparent, cylindrical, hermetically sealed glass tube was filled with 20 mL of fresh  $E^{\text{st}}$   
277 emulsion and placed in the measurement chamber of a Turbiscan MA2000 multiple light

278 scattering optical analyser Turbiscan MA2000 (Formulation, France). The tube was  
279 scanned at 50°C from top to bottom by a 850 nm light source and the back scattered light  
280 was recorded every 40  $\mu\text{m}$ . Analysis of the back scattered signal as a function of the height  
281 of the tube determined the total height of the emulsion (H) and the thickness of the creamed  
282 layer (h). The creaming ratio ( $r_c$ ) was defined as  $r_c = H/h$ . The measurements were performed  
283 on each E<sup>st</sup> emulsion after 0, 7, 14 and 21 days of storage at 50°C.

#### 284 **2.6.10 Surface protein concentration**

285 The method of separation of the non-adsorbed proteins from the emulsion droplets was  
286 derived from Patton & Huston, (1986). Forty-four milliliters of E<sup>st</sup> emulsion were gently mixed  
287 with 5 g saccharose in 50 mL centrifuge tubes and maintained at 50°C in a water bath. The  
288 tubes were centrifuged at 200 g for 20 min at 50°C and frozen at - 20°C. The frozen tubes  
289 were cut at the interface to separate the creamed milkfat droplets at the top of the tube and  
290 the aqueous phase containing saccharose and non-adsorbed caseins at the bottom. The  
291 milkfat droplet phases were transferred to other centrifuged tubes, melted at 50°C and  
292 redispersed in 15 mL of 4% (w/w) SDS solution. The tubes were centrifuged at 1 500 g for 20  
293 min at 50°C, frozen at - 20°C and cut to separate the top milkfat phase from the bottom  
294 aqueous SDS phase containing the adsorbed caseins. The first bottom saccharose aqueous  
295 phase (containing the non-adsorbed caseins) and the second bottom aqueous SDS phase  
296 (containing the adsorbed proteins) were both analyzed in terms of protein concentration  
297 using Kjeldahl and micro-Kjeldahl methods, respectively. The amounts of casein adsorbed at  
298 the interfaces were related to the specific surface areas of the droplets (previously  
299 determined by laser light diffraction) to calculate the interfacial casein concentrations and the  
300 percentages of adsorbed caseins.

#### 301 **2.7 Statistics**

302 Measurements were carried out on each of the replicates of suspensions S1<sub>d</sub>, S2<sub>d</sub>, S3<sub>d</sub> and  
303 S4<sub>d</sub>, emulsions E1<sup>ec</sup>, E2<sup>ec</sup>, E3<sup>ec</sup> and E4<sup>ec</sup> and emulsions E1<sup>st</sup>, E2<sup>st</sup>, E3<sup>st</sup> and E4<sup>st</sup>, except for

304 AsFIFFF,  $\gamma$  and dilatational rheology measurements. The standard deviations were  
305 calculated for each determination.

### 306 **3 Results**

307 The results are presented in two steps with first a focus on the physico-chemical and  
308 colloidal characteristics of the CAs in suspensions only. Their functional properties are then  
309 described when used as emulsifying agents in our model dairy emulsions.

#### 310 **3.1 Physicochemical characterization of casein aggregate suspensions**

##### 311 **3.1.1 Mineral characteristics**

312 Colloidal calcium and inorganic phosphate concentrations (Table 1) decreased  
313 simultaneously and in a correlated fashion (Fig. 2) in the order:  $S1_d < S2_d < S3_d < S4_d$ . This  
314 progressive casein micelle demineralization, expressed as a calcium demineralization rate  
315 (Table 1), was 24, 35, 56 and 81% for suspensions  $S1_d$ ,  $S2_d$ ,  $S3_d$  and  $S4_d$ , respectively.

316 On the other hand, the concentration of colloidal sodium (Table 1) increased in the  
317 suspensions with the increase in added TSC. This increase was correlated with the decrease  
318 in colloidal calcium concentration (Fig. 2), and therefore with the decrease in inorganic  
319 phosphate concentration. The chloride ions were only diffusible in the CA suspensions  
320 (Table 1). The sodium and chloride present in the saturated dialysis baths (counter ions of  
321 phosphate and calcium) mainly contributed to the high colloidal and diffusible concentrations  
322 observed in the dialyzed CA suspensions.

323 Magnesium and potassium were not present in the CA suspensions because these ions  
324 were not present in the purified casein micelles. Diffusible ion concentrations (Table 1) were  
325 similar in the suspensions and no diffusible or colloidal citrate was found after the dialysis  
326 step. Diffusible calcium was close to zero for all suspensions.

##### 327 **3.1.2 Colloid characterization**

328 Hydration of the ultracentrifugation pellets was constant for  $S1_d$ ,  $S2_d$  and  $S3_d$  and slightly  
329 lower for  $S4_d$  (Table 2). The concentration of sedimentable proteins decreased with the  
330 increase in the amount of TSC added and a reduction of 82% was found when comparing



331 suspension S1<sub>d</sub> with S4<sub>d</sub> (Table 2). The non-sedimentable casein content thus increased from  
332 8 to 18 g kg<sup>-1</sup> with the addition of TSC to the CA suspensions (Table 2).

333 Similar zeta potentials ( $22.7 \pm 1.3$  mV) were measured for each CA suspension (Table 2).

334 The UV, Rayleigh ratio and the calculated MW and R<sub>h</sub> of the CAs in the suspensions  
335 obtained by AsFIFFF are represented as a function of elution time, respectively (Fig. 3). For  
336 each suspension, three peaks that corresponded to three different populations of particles  
337 (A, B and C) were observed by UV:

338 Population A (19 - 27 min) corresponded to particles with MW from  $7.5 \times 10^7$  to  $2.5 \times 10^9$  g  
339 mol<sup>-1</sup> in S1<sub>d</sub>, S2<sub>d</sub> and R<sub>h</sub> from 30 to 100 nm. Population A in S4<sub>d</sub> had MW ranging from  $2.2 \times$   
340  $10^7$  to  $3.7 \times 10^9$  g mol<sup>-1</sup>, and R<sub>h</sub> between 130 and 250 nm. Differences between population A  
341 in S4<sub>d</sub> and in the other samples must be interpreted with caution because the Rayleigh ratio  
342 for this population in S4<sub>d</sub> was weak and the MW and R<sub>h</sub> values deduced from this signal  
343 might be less accurate. Moreover, according to the UV and Rayleigh ratio signals, the largest  
344 particles of S4<sub>d</sub> suspensions were eluted simultaneously with the largest particles of other  
345 suspensions, i.e. S1 and S2<sub>d</sub> (peaks are superimposed), and therefore these particles had  
346 similar MW and R<sub>h</sub>.

347 Population B particles (15.5 – 17 min) had R<sub>h</sub> between 21 and 26 nm (evaluated on S1<sub>d</sub> and  
348 S2<sub>d</sub> only). Corresponding MW were between  $1.4 \times 10^7$  and  $3.15 \times 10^7$  for S1<sub>d</sub> and S2<sub>d</sub> and  
349 between  $3.4 \times 10^6$  and  $1 \times 10^7$  for S4<sub>d</sub>. Finally, population C (14-15 min) had R<sub>h</sub> between 18  
350 and 22 nm (evaluated on S1<sub>d</sub> and S2<sub>d</sub> only) and MW between  $7.0 \times 10^6$  and  $1.5 \times 10^7$  g.mol<sup>-1</sup>  
351 for S1<sub>d</sub> and S2<sub>d</sub> and between  $1.4 \times 10^6$  and  $3.4 \times 10^6$  for S4<sub>d</sub>. As for population A, differences  
352 between MW in S4<sub>d</sub> and in the other samples must be interpreted with caution. Again, UV  
353 signals indicated that for all suspensions, the B and C populations of particles eluted  
354 simultaneously in S1<sub>d</sub>, S2<sub>d</sub>, and S4<sub>d</sub>. According to the quality of the Rayleigh ratios signals of  
355 the suspensions, different data treatments were applied which could explain the differences  
356 in the MW values observed.

357 The proportions of the different populations of particles depended on the amount of added  
358 TSC: the largest particles (A) disappeared when the TSC concentration increased, permitting  
359 the appearance of the two smallest populations (B and C). Nevertheless, the loss in surface  
360 area under the A peak was not equal to the gain in surface area under the B and C peaks  
361 due to the fact that the largest particles not only absorbed but also diffused the UV signal  
362 compared to small particles that only absorbed the UV signal.

### 363 **3.2 Functional characterization of casein aggregate suspensions**

#### 364 **3.2.1 Emulsifying capacity of casein aggregate suspensions**

365 The particle size distribution profiles of E1<sup>ec</sup>, E2<sup>ec</sup>, E3<sup>ec</sup> and E4<sup>ec</sup> emulsions are presented in  
366 Figure 4. Given that the size distribution profiles were monomodal, the mode values (*i.e.* the  
367 maximum of each peak) are represented as a function of the added TSC concentration in the  
368 CA suspensions (Fig. 4C empty symbols). The distributions shifted to smaller sizes (Fig. 4A,  
369 C) as the added TSC concentration increased in the CA suspensions and the mode values  
370 varied between 27 and 14  $\mu\text{m}$ . This size range corresponded to macro emulsions. In the  
371 presence of SDS, the size distributions of the particles were smaller and narrower than in the  
372 absence of SDS (Fig. 4), revealing aggregation of the emulsion droplets. The mean diameter  
373 of the emulsion droplets decreased as a function of the increase in TSC concentration in the  
374 CA suspension (Fig 4). Figure 5 shows confocal micrographs of the fresh E1<sup>ec</sup>, E2<sup>ec</sup>, E3<sup>ec</sup> and  
375 E4<sup>ec</sup> emulsions. Milkfat droplets (in red) were surrounded by casein aggregates (in green).  
376 Microstructural observations confirmed the decrease in the size of the emulsion droplets as a  
377 function of the increase in TSC concentration in the CA suspensions. Moreover, flocculation  
378 of the emulsion droplets was characterized in each emulsion, in agreement with particle size  
379 measurements (Fig. 4).

380 The interfacial tension ( $\gamma$ ) at the melted milk fat/CA suspension interface was measured to  
381 evaluate the activity of the CAs at the milkfat droplet surface. Blank interfacial tension  
382 determined on the last dialysis bath of the CA suspensions was 10  $\text{mN m}^{-1}$ . The presence of  
383 CAs decreased  $\gamma$  to around 5 - 6  $\text{mN m}^{-1}$  whatever the added TSC concentration.

### 384 3.2.2 Emulsion-stabilizing capacity of the casein aggregate suspensions

385 The evolution of the creaming ratios ( $r_c$ ) of E<sup>st</sup> emulsions over time are shown in Figure 6.

386 None of the emulsions were stable against creaming. Phase separation was easily  
387 observable after 7 days of storage and did not vary during the following 14 days. The  
388 determination of  $r_c$  indicated that the thickness of the creamed layers decreased with the  
389 increase in added TSC in the CA suspensions.

390 Laser light scattering measurements and confocal microscopy observations were performed  
391 on each emulsion throughout storage at 50°C (Fig. 7). Given that the particle size distribution  
392 profiles were monomodal (data not shown), the evolution of the mode value of each emulsion  
393 as a function of time is represented. The light scattering measurements were carried out in  
394 the presence and absence of SDS. Indeed, this small surfactant is able to dissociate  
395 flocculated droplets by replacing the protein at interfaces, permitting discrimination of  
396 flocculated droplets from coalesced droplets. When droplets flocculated, the emulsion size  
397 distribution shifted to smaller sizes (smaller mode value). In contrast, the addition of SDS had  
398 no influence on the size distribution of coalesced droplets. Figure 7 shows that the size of the  
399 particles in emulsions increased with time without SDS, especially for emulsions from CA  
400 suspensions containing TSC. For example, the mode value of E2<sup>st</sup> increased from 12 to 33  
401  $\mu\text{m}$  after 21 days of storage and from 12 to 90  $\mu\text{m}$  for E4<sup>st</sup>. In the presence of SDS, the size  
402 distribution of the droplets did not evolve over time, the mode being 12  $\mu\text{m}$ , similar to the size  
403 determined after the preparation of the emulsions (data not shown). These constant values  
404 indicated that E2<sup>st</sup>, E3<sup>st</sup> and E4<sup>st</sup> were destabilized by flocculation but were stable against  
405 coalescence. The E1<sup>st</sup> emulsion, which maintained a constant mode value throughout  
406 storage, was stable against both flocculation and coalescence phenomena.

407 The corresponding micrographs of each emulsion at each time-point were in good  
408 agreement with laser light scattering data (Fig. 7). Each emulsion maintained the same  
409 droplet size during storage. However, some micrographs showed contrast differences, with  
410 bright milkfat droplets at the foreground of the image and dark red droplets at the back. This

411 color variation was attributed to the appearance of 3D milkfat droplet flocs in the emulsions  
412 that coexisted on different focal planes of the micrographs. According to the microscopy  
413 observations, E3<sup>st</sup> and E4<sup>st</sup> emulsions were the most highly flocculated under our storage  
414 conditions.

415 The zeta potential of individual emulsion droplets and flocculated droplets did not evolve  
416 significantly during the 21 days of storage ( $23.1 \pm 1.4$  mV).

417 Around  $24 \pm 1\%$  of the total protein present in the emulsions was adsorbed at the interface,  
418 whatever the type of CA suspension used to make the emulsion, which corresponded to a  
419 casein surface concentration of around  $17.4 \pm 0.7$  mg m<sup>-2</sup>.

420 The interfacial dilatational moduli ( $E^*$ ,  $E'$  and  $E''$ ) were determined at the melted milkfat/CA  
421 suspensions interface. All suspensions presented similar values:  $14.6 \pm 0.4$ ,  $14.4 \pm 0.4$  and  
422  $2.9 \pm 0.2$  for complex ( $E^*$ ), elastic ( $E'$ ) and viscous ( $E''$ ) moduli, respectively. The contribution  
423 of  $E'$  to  $E^*$  was higher than the  $E''$  contribution, reflecting solid-like behavior of the adsorbed  
424 casein aggregate layers.

425

## 426 **4 Discussion**

427 The results are discussed in two stages, with first a focus on the characterization of the CA  
428 suspensions in terms of mineralization and colloidal properties. The second stage consisted  
429 of investigation of the emulsifying and emulsion-stabilizing capacity of the CA used as  
430 emulsifying agents in two types of model dairy emulsions.

### 431 **4.1 Characterization of the different CA suspensions**

#### 432 **4.1.1 Addition of TSC resulted in progressive casein micelle demineralization**

433 Analysis of the distribution of minerals confirmed that TSC had an influence on the  
434 mineralization of the casein micelle. By chelating the diffusible calcium, citrate ions induced  
435 the progressive removal of the colloidal calcium (Gaucheron, 2004). This was in accordance  
436 with results reported by many authors who recorded citrate chelation of calcium either by  
437 determining calcium activity (de Kort et al., 2011; Johnston & Murphy, 1992; Udabage,  
438 McKinnon, & Augustin, 2001), or diffusible calcium and/or colloidal calcium concentrations  
439 (Le Ray et al., 1998; Mizuno & Lucey, 2005; Mohammad & Fox, 1983; Odagiri & Nickerson,  
440 1965; Ozcan-Yilsay, Lee, Horne, & Lucey, 2007; Vujcic, deMan, & Woodrow, 1968) in milk  
441 or micellar suspensions.

442 The simultaneous and correlated decrease in the colloidal inorganic phosphate concentration  
443 (Fig. 2) was attributed to the solubilization of the colloidal calcium phosphate (Le Ray et al.,  
444 1998; Mizuno & Lucey, 2005; Mohammad & Fox, 1983). Increasing the concentration of TSC  
445 therefore led to progressive calcium phosphate demineralization of the CA suspensions.

446 Furthermore, the correlation observed between the colloidal concentrations of calcium and  
447 sodium (Fig. 2) suggested that the negative charges induced by the calcium demineralization  
448 (presence of free phosphoserine residues) were screened by monovalent sodium ions,  
449 potentially explaining the constant zeta potential observed for each CA suspension (Table 2).

450 Mineral content was also modified by the casein powder resuspension and dialysis steps.

451 Determination of colloidal and diffusible calcium in S1 (prior to dialysis – data not shown) and  
452 S1<sub>d</sub> (after dialysis) induced partial solubilization of the colloidal calcium. This limited calcium

453 demineralization (24%, reported in Table 1) was attributed to the resuspension of the purified  
454 casein micelle powder in water and to the dialysis step.

455 The dialysis step also permitted removal of the added citrate and established a similar  
456 diffusible phase in the four suspensions (Table 1). As the result, the ionic strengths of all the  
457 suspensions were taken to be similar in the four suspensions.

#### 458 **4.1.2 TSC demineralization resulted in disaggregation of the casein micelle**

459 Structural modifications of the CA were observed parallel to the micellar demineralization.  
460 The quantity of sedimentable proteins was reduced and that of non-sedimentable proteins  
461 consistently increased (Table 2), which showed progressive dissociation of the CAs. Similar  
462 trends were reported by Udabage et al. (2001), Le Ray et al. (1998) and De Kort et al.  
463 (2011).

464 AsFIFFF characterization was performed in order to evaluate the sizes of the dissociated  
465 CAs. This revealed that three populations of particles of different sizes and proportions were  
466 simultaneously present in the CA suspensions (Fig. 3). Population A consisted of large CA  
467 with MW and  $R_h$  comparable to those of the casein micelle (MW between  $5 \times 10^7$  and  $1 \times 10^{10}$   
468  $\text{g}\cdot\text{mol}^{-1}$  and  $r_{\text{rms}}$  of 50 – 350 nm), as previously reported (Glantz, Håkansson, Lindmark  
469 Månsson, Paulsson, & Nilsson, 2010; Pitkowski et al., 2008). The addition of TSC induced  
470 dissociation of these aggregates and increased the proportion of population B. This  
471 population consisted of aggregates similar to sodium caseinate particles with MW of 4 to 9 x  
472  $10^6 \text{ g}\cdot\text{mol}^{-1}$  and  $R_h$  between in 10 – 20 nm, as reported by Lucey, Srinivasan, Singh, & Munro  
473 (2000). Using 50 times more TSC per gram of protein than in our study, Panouillé et al.  
474 (2004) reported slightly smaller CAs (MW =  $2 \times 10^5 \text{ g}\cdot\text{mol}^{-1}$  and  $R_h = 12 \text{ nm}$ ). Finally,  
475 population C corresponded to the smallest particles in our suspensions. The percentage of  
476 these small particles was also increased by the increased addition of TSC. This suggested  
477 that population C corresponded to casein monomers dissociated from the larger CAs.  
478 According to Guyomarc'h et al. (2010) and Glantz et al (2010), they could also be attributed  
479 to residual whey protein monomers.

480 As demonstrated by Pitkowski, Nicolai, & Durand (2007), Lin, Leong, Dewan, Bloomfield, &  
481 Morr (1972) and Marchin et al. (2007) with polyphosphate and EDTA calcium chelation, the  
482 dissociation of casein micelles by calcium chelating agents is a “cooperative process” in  
483 which the structure of the casein micelle remains intact (large aggregates) or becomes fully  
484 dissociated (small aggregates of the same size are produced). In other words, the  
485 dissociation of the casein micelle does not provide aggregates of intermediate sizes. The  
486 three populations of particles (casein micelle-like aggregates, sodium caseinate-like  
487 aggregates, and protein monomers) and their dependence on the amount of TSC added  
488 confirmed that the “cooperative process” can be applied to the TSC dissociation of casein  
489 micelles.

490 The hydration measurements of S1<sub>d</sub>, S2<sub>d</sub>, S3<sub>d</sub> and S4<sub>d</sub> pellets (Table 2) differed from the  
491 findings of Le Ray et al. (1998) who reported that the water content of the sedimented CAs  
492 increased with the addition of TSC. This was also supported by the voluminosity data  
493 determined by De Kort et al. (2011). Compared to our study, these authors did not monitor  
494 the diffusible phases of their suspensions. The dialysis step and thus the diffusible  
495 environment of the sedimentable casein aggregates therefore seemed to have an impact on  
496 their hydration.

497 As expected, TSC demineralized and dissociated the casein micelle to different extents in  
498 order to produce four suspensions containing various CAs. The effects of a calcium chelating  
499 agent on the casein micelle seemed to be in good agreement with the use of an ion-  
500 exchange resin to sequester the calcium ((Xu et al., 2016; Ye, 2011). Xu et al., (2016)  
501 reported a similar dissociation of the casein micelle into smaller CAs and a decrease in the  
502 total calcium content of their casein micelle suspension. These authors also reported that,  
503 beyond a level of 20% of calcium demineralization (which is lower than the demineralization  
504 rate of our four suspensions), the dissociated caseins present in the ultracentrifuged  
505 supernatant (non-sedimentable proteins) were of similar composition to that of the native

506 casein micelle. This suggests that the micelle-like CAs and the mixture of sodium-caseinate  
507 CAs and the “free” casein monomers have the same composition.

508 This first step of our study was necessary to characterize and control our CA suspensions  
509 accurately in order to elucidate their emulsifying and emulsion-stabilizing capacity. To  
510 summarise, suspension S1<sub>d</sub> mostly contained highly mineralized and large casein micelle-like  
511 CAs. Intermediate suspensions (S2<sub>d</sub> and S3<sub>d</sub>) contained a mixture of both large and small  
512 sodium caseinate-like CAs, with a small quantity of “free” casein monomers. Finally, S4<sub>d</sub>  
513 mainly consisted of poorly mineralized small CAs, “free” casein monomers and residual  
514 traces of large CAs (Fig. 8A).

## 515 **4.2 Investigation of CA capacity as emulsifying agents**

### 516 **4.2.1 Decreasing the size of the CA increased its emulsifying capacity**

517 The emulsifying capacity of a protein (or a protein aggregate) can be characterized by  
518 measuring the emulsion droplet size at a particular protein concentration: the smaller the  
519 droplet, the better the protein aggregate as an emulsifier (Euston & Hirst, 1999). Differences  
520 in emulsifying capacity can generally be attributed to the surface activity and/or to the size of  
521 the emulsifying agent: the higher the surface activity and/or the smaller the size, the greater  
522 the emulsifying capacity.

523 Emulsion size distribution profiles and micrographs (Figs. 4, 5) clearly indicated differences  
524 in emulsifying capacity which depended on the CA suspension used. The presence of small  
525 CAs facilitated the blending of the milkfat, making it possible to form emulsions with a smaller  
526 droplet size, and protected the emulsions against the appearance of bridging flocculation  
527 between the milkfat droplets (Fig. 8B).

528 The surface tension,  $\gamma$ , is characteristic of the surface activity of the CA, *i.e.* how effective  
529 CAs are at reducing unfavorable interactions between the milkfat and the suspension  
530 (McClements, 2005). For the concentrations used here, the surface tension measurements  
531 at the milk fat/CA suspension interfaces revealed that large micelle-like and small sodium  
532 caseinate-like CAs had the same ability to reduce the unfavorable interactions between the



533 two phases ( $5 - 6 \text{ mN m}^{-1}$ ). All the samples had the same surface tension at equilibrium  
534 (obtained after 5 min) and hence the same surface coverage.

535 Our results, showing that there was no difference in equilibrium between our samples,  
536 differed from those of Courthaudon et al. (1999), who found that sodium caseinate was more  
537 surface active than casein micelles. However, this strongly depends on the concentrations  
538 studied: in the study reported here we used a fairly high concentration (20 g/kg) and the  
539 interfacial layer was obtained at equilibrium by the combined adsorption of the free casein  
540 monomers, the sodium caseinate-like CAs and the micelle-like CAs, which ruptured once  
541 adsorbed. Indeed, measurements at a concentration of 1.2 g/kg also provided the same  
542 surface tensions and rheological properties (whatever the state of aggregation – data not  
543 shown), meaning that at a concentration of 20 g/kg there was a large reservoir of proteins in  
544 the bulk, compared to the quantity that could be adsorbed.

545 It is not possible from these measurements to simply ascribe the differences in emulsifying  
546 properties to different surface activities of the types of aggregates. Nevertheless, as we also  
547 report here, Courthaudon et al (1999), Ye (2011), Mulvihill & Murphy (1991) and Euston &  
548 Hirst (1999) established a correlation between the state of aggregation of the caseins and  
549 their emulsifying capacity.

550 For further analysis, it is important to note that we were not able to monitor the dynamics of  
551 adsorption at short timescales  $t$  (typically for  $t < 2 \text{ s}$ ). However, our results showed that the  
552 surface tension had already decreased significantly during this short non-monitored period.  
553 There might therefore have been differences in the dynamics of adsorption between the  
554 samples at very short timescales (those having the highest concentrations of monomers  
555 reducing the surface tension more rapidly).

556 In fact, the emulsion production process was rapid, and the associated timescale was also in  
557 the order of 1 s. Understanding the differences between emulsifying properties may therefore  
558 require monitoring of the surface coverage at such short timescales (less than 1 s). Many  
559 small, mobile casein units, such as casein monomers and sodium caseinate-like CAs are

560 thus available for rapid adsorption and to emulsify greater amounts of milkfat/suspension  
561 interface at high concentrations of TSC. In contrast, when not enough casein units were  
562 present in the suspension to adsorb on the generated interface rapidly (e.g. E1<sup>ec</sup>), the milkfat  
563 droplets coalesced until all their surfaces were covered, thus making the emulsions coarser.  
564 Large micelle-like CAs also had the ability to share between two independent droplets and  
565 induce bridging flocculation (Fig. 8B).

#### 566 **4.2.2 Emulsions were stable against coalescence but creamed and flocculated**

567 Destabilization of emulsions can result from three phenomena i.e. creaming, flocculation and  
568 coalescence. The E<sup>st</sup> emulsions were designed to have identical droplet sizes, despite the  
569 differences in CA suspension emulsifying capacity used to prepare them. This approach  
570 removed the influence of the droplet size on the creaming, flocculation and coalescence  
571 phenomena.

572 Visual observations (Fig. 6) and emulsion size measurements (Fig. 7) as a function of time  
573 showed that the emulsions remained stable against coalescence throughout storage.

574 However, emulsions were destabilized by creaming and flocculation (Fig. 7).

#### 575 **4.2.3 The adsorbed CAs contributed to coalescence stability whatever their state of** 576 **aggregation.**

577 The stability of the emulsions against coalescence is generally correlated with the  
578 characteristics of the CA layers adsorbed at the droplet surface. Interfacial casein  
579 concentrations and surface tension values provided information on the extent of casein  
580 adsorption at the interface, and dilational rheology determined how strongly proteins were  
581 adsorbed and interacted at the interface (McClements, 2005).

582 As with the surface tension data, the surface casein concentrations were also similar (17.4  
583 mg m<sup>-2</sup>) and independent of the type of CA used to form each emulsion. Our values were  
584 between those found by Euston & Hirst (1999) on milk casein concentrate (21 mg m<sup>-2</sup>) and  
585 Courthaudon et al. (1999) on casein micelles (10 mg m<sup>-2</sup>). Our values were 6 to 8 times

586 higher than the values reported for sodium caseinate ( $2.3 \text{ mg m}^{-2}$  by Euston & Hirst (1999),  
587  $3 \text{ mg m}^{-2}$  by Dickinson, Golding & Povey (1997),  $1 \text{ mg m}^{-2}$  by Dickinson & Golding (1997) and  
588  $1.63 \text{ mg m}^{-2}$  by Courthaudon et al (1999)). Our measurements thus fall within the highest  
589 reported values for interfacial concentration, and can be interpreted as a thick layer of  
590 adsorbed proteins, in agreement with the fact that we were using high protein concentrations,  
591 such that the interfacial properties did not depend on the concentration and that we had a  
592 large excess of proteins in bulk.

593 Dilatational rheology measurements demonstrated that adsorbed layers of CAs had similar  
594 solid-like behaviors ( $E' \gg E''$ ) whatever the state of aggregation of the casein used to form  
595 the emulsion. Large CAs spread out at the interface, and intermolecular interactions within  
596 the adsorbed layers were similar. The wide contribution of  $E'$  to  $E^*$  ( $E \gg E''$ ) was in  
597 agreement with the literature on sodium caseinate at diverse oil/water interfaces (Amine,  
598 Dreher, Helgason, & Tadros, 2014; Benjamins, Cagna, & Lucassen-Reynders, 1996). These  
599 two results suggested that the state of aggregation of the casein was not decisive for the  
600 stability of the emulsions against coalescence.

#### 601 **4.2.4 Creaming and flocculation enhanced each other**

602 Creaming is due to the difference in density between the milkfat and the aqueous suspension  
603 phases of the emulsions. This phenomenon was enhanced by the large size of the individual  
604 milkfat droplets ( $12 \mu\text{m}$ ). In our case, creaming (Fig. 6) and flocculation (Fig. 7) only occurred  
605 during the first week of storage, suggesting that these two concomitant phenomena  
606 influenced each other. On the one hand, creaming was intensified by the formation of milkfat  
607 droplet combination due to flocculation. On the other hand, flocculation was favored by the  
608 creaming that moved the droplets forward and encouraged their contact, which is a  
609 necessary step for the final destabilization of flocculation to occur (Dauphas, Amestoy,  
610 Llamas, Anton, & Riaublanc, 2008). However, the nature of the CA and the environment also  
611 had a role in the appearance of flocculation.

#### 612 **4.2.5 Unabsorbed CAs induced depletion-flocculation of the emulsion droplets**

613 Depletion-flocculation is an instability mechanism that occurs in emulsions and is induced by  
614 the presence of unabsorbed particles. It takes place when two neighboring droplets are close  
615 enough to exclude any unabsorbed particles from the gap that separates them.

616 Consequently, an osmotic pressure gradient is induced that causes net attraction between  
617 the emulsion droplets (Asakura & Oosawa, 1958; Dickinson & Golding, 1997, 1998;  
618 Dickinson et al., 1997; Radford & Dickinson, 2004). This phenomenon was observed in our  
619 emulsions because of the presence of unabsorbed CAs.

620 The evolution of the milkfat droplet sizes in the emulsion as a function of time (Fig. 7)  
621 revealed that increases in percentage of small CAs in the emulsions augmented flocculation  
622 of the milkfat droplets. This was in agreement with the results obtained on native casein  
623 micelles, calcium-depleted casein micelles, calcium caseinate and sodium caseinate  
624 (Dickinson & Golding, 1998; Euston & Hirst, 1999; Srinivasan, Singh, & Munro, 2001; Ye,  
625 2011). These reported studies demonstrated that the depletion-flocculation process was  
626 strongly dependent on the state of aggregation of the casein. Furthermore, small CAs were  
627 of the optimum size (20 nm) to cause the greatest depletion-flocculation of emulsion droplets  
628 (Radford & Dickinson, 2004).

#### 629 **4.2.6 CA environment (mineral equilibrium and storage temperature) influenced the** 630 **sticking of the emulsion droplets**

631 Finally, storage temperatures higher than 37°C can induce gelation by flocculation of sodium  
632 caseinate and  $\beta$  casein emulsions if a sufficient amount of added calcium is present in the  
633 emulsion aqueous phase (Dauphas et al., 2008; Dickinson & Casanova, 1999; Dickinson &  
634 Eliot, 2003; Eliot & Dickinson, 2003). Added calcium reduces the steric repulsion between  
635 the emulsion droplets by binding to the adsorbed caseins, and high temperature encourages  
636 hydrophobic interactions between caseins and promotes sticking behavior (Dauphas et al.,  
637 2008; Dickinson & Casanova, 1999). However, no calcium was present in the diffusible  
638 phases of the emulsions as it was not present in the CA suspensions (Table 1). Moreover,

639 the extent of flocculation increased when the colloidal calcium content of the CAs decreased.  
640 This suggested that sodium ions reduced steric repulsion between the emulsion droplets in  
641 our system. This hypothesis was supported by the increased colloidal sodium content in the  
642 CA suspensions (Table 1) and the constant zeta potential values ( $23.1 \pm 1.4$  mV) measured  
643 on  $E^{st}$  emulsions throughout storage. Because of their highly aggregated state, large and  
644 strongly mineralized CAs were also less inclined to link with their counterparts adsorbed on  
645 separated milkfat droplets or suspended in the bulk emulsion phases.

646

**5 Conclusion**

Varying the concentration of added TSC in pure casein micelle suspensions produced four CA suspensions that were progressively demineralized and dissociated. The diffusible phases of these suspensions were monitored with a dialysis step. The use of these CAs as emulsifying agents in our model dairy emulsions revealed differences in emulsifying and emulsion-stabilizing properties. The smaller CAs had better emulsifying capacity as their presence favored the formation of emulsions with smaller droplet sizes. The surface activity of the four CA suspensions was similar and the differences in emulsifying capacity were attributed only to variation of the state of aggregation of the CAs. With regard to the stabilizing capacity of the CAs, all the emulsions were unstable under our storage conditions (21 days, 50°C). Creaming was promoted by the presence of large droplets in the emulsions and favored the occurrence of flocculated droplets. Flocculation was also enhanced by the presence of small, demineralized CAs. However, all the emulsions remained stable against coalescence during storage. This was probably due to the presence of similar quantities of adsorbed CAs at the surface of the emulsion droplets that formed protective layers with similar viscoelastic properties. Combining the results obtained on the CAs in suspension with the emulsion properties revealed that the state of aggregation of the CAs had a major impact on their emulsifying capacity and emulsion-stabilizing properties. Modulating the mineral content of the casein micelle is therefore an interesting method for optimization of emulsion functionality. Further studies on CA composition and nanostructure, both in suspension and adsorbed at the milkfat/water interface, would improve understanding of the differences between the emulsifying and emulsion-stabilizing properties. In this case, the destabilization of the emulsions in the early stages should be studied for a better understanding of the involved phenomena. As an extension of this work, investigation of the rheology of the creamed layers of the emulsions is planned as well as the assessment of other functionalities of newly formed CAs.

673 **Acknowledgements:**

674 The authors thank the French Dairy Interbranch Organization (CNIEL) for their financial  
675 support, Rachel Boutrou for assistance with writing the manuscript and Anne-Laure Chapeau  
676 for proof reading the article.

677 **References:**

- 678 Amine, C., Dreher, J., Helgason, T., & Tadros, T. (2014). Investigation of emulsifying  
679 properties and emulsion stability of plant and milk proteins using interfacial tension  
680 and interfacial elasticity. *Food Hydrocolloids*, 39, 180–186.
- 681 Asakura, S., & Oosawa, F. (1958). Interaction between particles suspended in solutions of  
682 macromolecules. *Journal of Polymer Science*, 33 ,(126), 183–192.
- 683 Barbosa-Cánovas, G. V., Kokini, J. L., Ma, L., & Ibarz, A. (1996). The Rheology of  
684 Semiliquid Foods. In *Advances in Food and Nutrition Research* (Vol. 39, pp. 1–69).  
685 Elsevier.
- 686 Benjamins, J., Cagna, A., & Lucassen-Reynders, E. H. (1996). Viscoelastic properties of  
687 triacylglycerol/water interfaces covered by proteins. *Colloids and Surfaces A:  
688 Physicochemical and Engineering Aspects*, 114, 245–254.
- 689 Broyard, C., & Gaucheron, F. (2015). Modifications of structures and functions of caseins: a  
690 scientific and technological challenge. *Dairy Science & Technology*.
- 691 Brulé, G., Maubois, J.-L., & Fauquant, J. (1974). Etude de la teneur en éléments minéraux des  
692 produits obtenus lors de l'ultrafiltration du lait sur membrane. *Lait*, (539-540), 600 –  
693 615.
- 694 Courthaudon, J.-L., Girardet, J.-M., Campagne, S., Rouhier, L.-M., Campagna, S., Linden, G.,  
695 & Lorient, D. (1999). Surface active and emulsifying properties of casein micelles  
696 compared to those of sodium caseinate. *International Dairy Journal*, 9(3–6), 411–412.

- 697 Dalgleish, D. G., & Corredig, M. (2012). The structure of the casein micelle of milk and its  
698 changes during processing. *Annual Review of Food Science and Technology*, 3 (1),  
699 449–467.
- 700 Dauphas, S., Amestoy, M., Llamas, G., Anton, M., & Riaublanc, A. (2008). Modification of  
701 the interactions between  $\beta$ -casein stabilized oil droplets with calcium addition and  
702 temperature changing. *Food Hydrocolloids*, 22(2), 231–238.
- 703 de Kort, E., Minor, M., Snoeren, T., van Hooijdonk, T., & van der Linden, E. (2011). Effect  
704 of calcium chelators on physical changes in casein micelles in concentrated micellar  
705 casein solutions. *International Dairy Journal*, 21(12), 907–913.
- 706 Dickinson, E. (1999). Caseins in emulsions: interfacial properties and interactions.  
707 *International Dairy Journal*, 9(3-6), 305–312.
- 708 Dickinson, E., & Casanova, H. (1999). A thermoreversible emulsion gel based on sodium  
709 caseinate. *Food Hydrocolloids*, 13(4), 285–289.
- 710 Dickinson, E., & Eliot, C. (2003). Defining the conditions for heat-induced gelation of a  
711 caseinate-stabilized emulsion. *Colloids and Surfaces B: Biointerfaces*, 29(2-3), 89–97.
- 712 Dickinson, E., & Golding, M. (1997). Depletion flocculation of emulsions containing  
713 unabsorbed sodium caseinate. *Food Hydrocolloids*, 11(1), 13–18.
- 714 Dickinson, E., & Golding, M. (1998). Influence of calcium ions on creaming and rheology of  
715 emulsions containing sodium caseinate. *Colloids and Surfaces A: Physicochemical  
716 and Engineering Aspects*, 144(1-3), 167–177.
- 717 Dickinson, E., Golding, M., & Povey, M. J. W. (1997). Creaming and flocculation of oil-in-  
718 water emulsions containing sodium caseinate. *Journal of Colloid and Interface  
719 Science*, 185(2), 515–529.
- 720 Eliot, C., & Dickinson, E. (2003). Thermoreversible gelation of caseinate-stabilized  
721 emulsions at around body temperature. *International Dairy Journal*, 13(8), 679–684.



- 722 Euston, S. R., & Hirst, R. L. (1999). Comparison of the concentration-dependent emulsifying  
723 properties of protein products containing aggregated and non-aggregated milk protein.  
724 *International Dairy Journal*, 9(10), 693–701.
- 725 Foegeding, E. A., & Davis, J. P. (2011). Food protein functionality: a comprehensive  
726 approach. *Food Hydrocolloids*, 25(8), 1853–1864.
- 727 Gaucheron, F. (2004). *Minéraux et produits laitiers*. Paris: Technique & Documentation.
- 728 Gaucheron, F., Le Graet, Y., Piot, M., & Boyaval, E. (1996). Determination of anions of milk  
729 by ion chromatography. *Le Lait*, 76(5), 433–443.
- 730 Glantz, M., Håkansson, A., Lindmark Månsson, H., Paulsson, M., & Nilsson, L. (2010).  
731 Revealing the size, conformation, and shape of casein micelles and aggregates with  
732 asymmetrical flow field-flow fractionation and multiangle light scattering. *Langmuir*,  
733 26(15), 12585–12591.
- 734 Guyomarc'h, F., Violleau, F., Surel, O., & Famelart, M.-H. (2010). Characterization of heat-  
735 induced changes in skim milk using asymmetrical flow field-flow fractionation  
736 coupled with multiangle laser light scattering. *Journal of Agricultural and Food*  
737 *Chemistry*, 58(24), 12592–12601.
- 738 Guzey, D., & McClements, D. J. (2006). Formation, stability and properties of multilayer  
739 emulsions for application in the food industry. *Advances in Colloid and Interface*  
740 *Science*, 128-130, 227–248.
- 741 Holt, C., Carver, J. A., Ecroyd, H., & Thorn, D. C. (2013). Caseins and the casein micelle:  
742 their biological functions, structures, and behavior in foods. *Journal of Dairy Science*,  
743 96(10), 6127–6146.
- 744 Holt, C., & Horne, D. S. (1996). The hairy casein micelle: evolution of the concept and its  
745 implications for dairy technology. *Nederlands Melk En Zuiveltijdschrift*, 50(2), 85 –  
746 111.

- 747 International Dairy Federation. (1993). Lait et crème en poudre - Détermination de la teneur  
748 en eau. International Standard FIL-IDF 26A
- 749 International Dairy Federation. (2014). Milk and milk products - Determination of nitrogen  
750 content - Part 1: Kjeldahl principle and crude protein calculation.
- 751 Johnston, D. E., & Murphy, R. J. (1992). Effects of some calcium-chelating agents on the  
752 physical properties of acid-set milk gels. *Journal of Dairy Research*, 59(02), 197.
- 753 Le Ray, C., Maubois, J.-L., Gaucheron, F., Brulé, G., Pronnier, P., & Garnier, F. (1998). Heat  
754 stability of reconstituted casein micelle dispersions: changes induced by salt addition.  
755 *Le Lait*, 78(4), 375–390.
- 756 Lin, S. H. C., Leong, S. L., Dewan, R. K., Bloomfield, V. A., & Morr, C. V. (1972). Effect of  
757 calcium ion on the structure of native bovine casein micelles. *Biochemistry*, 11(10),
- 758 Lopez, C., Bourgaux, C., Lesieur, P., & Ollivon, M. (2007). Coupling of time-resolved  
759 synchrotron X-ray diffraction and DSC to elucidate the crystallization properties and  
760 polymorphism of triglycerides in milk fat globules. *Le Lait*, 87(4-5), 459–480.
- 761 Lucey, J. A., Srinivasan, M., Singh, H., & Munro, P. A. (2000). Characterization of  
762 commercial and experimental sodium caseinates by multiangle laser light scattering  
763 and size-exclusion chromatography. *Journal of Agricultural and Food Chemistry*,  
764 48(5), 1610–1616.
- 765 Marchin, S., Putaux, J.-L., Pignon, F., & Léonil, J. (2007). Effects of the environmental  
766 factors on the casein micelle structure studied by cryo transmission electron  
767 microscopy and small-angle x-ray scattering/ultrasmall-angle x-ray scattering. *The*  
768 *Journal of Chemical Physics*, 126(4), 045101.
- 769 McClements, D. J. (2005). *Food emulsions principles, practices, and techniques*. Boca Raton:  
770 CRC Press.

- 771 Mizuno, R., & Lucey, J. A. (2005). Effects of emulsifying salts on the turbidity and calcium-  
772 phosphate–protein interactions in casein micelles. *Journal of Dairy Science*, 88(9),  
773 3070–3078.
- 774 Mohammad, K. S., & Fox, P. F. (1983). Influence of some polyvalent organic acids and salts  
775 on the colloidal stability of milk. *International Journal of Dairy Technology*, 36(4),  
776 112–117.
- 777 Mulvihill, D. M., & Murphy, P. C. (1991). Surface active and emulsifying properties of  
778 caseins/caseinates as influenced by state of aggregation. *International Dairy Journal*,  
779 1(1), 13–37.
- 780 Odagiri, S., & Nickerson, T. A. (1965). Complexing of calcium by hexametaphosphate,  
781 oxalate, citrate, and ethylenediamine-tetraacetate in milk. II. Dialysis of milk  
782 containing complexing agents. *Journal of Dairy Science*, 48(1), 19–22.
- 783 Ozcan-Yilsay, T., Lee, W.-J., Horne, D., & Lucey, J. A. (2007). Effect of trisodium citrate on  
784 rheological and physical properties and microstructure of yogurt. *Journal of Dairy*  
785 *Science*, 90(4), 1644–1652.
- 786 Panouillé, M., Nicolai, T., & Durand, D. (2004). Heat induced aggregation and gelation of  
787 casein submicelles. *International Dairy Journal*, 14(4), 297–303.
- 788 Patton, S., & Huston, G. E. (1986). A method for isolation of milk fat globules. *LIPIDS*,  
789 21(2), 170–174.
- 790 Pierre, A., Fauquant, J., Le Graet, Y., & Maubois, J.-L. (1992). Préparation de  
791 phosphocaséinate natif par microfiltration sur membrane. *Lait*, (72), 461 – 474.
- 792 Pitkowski, A., Durand, D., & Nicolai, T. (2008). Structure and dynamical mechanical  
793 properties of suspensions of sodium caseinate. *Journal of Colloid and Interface*  
794 *Science*, 326(1), 96–102.

- 795 Pitkowski, A., Nicolai, T., & Durand, D. (2007). Scattering and turbidity study of the  
796 dissociation of the casein by calcium chelation. *Biomacromolecules*, *9*, 369–375.
- 797 Radford, S. J., & Dickinson, E. (2004). Depletion flocculation of caseinate-stabilized  
798 emulsions: what is the optimum size of the non-adsorbed protein nano-particles?  
799 *Colloids and Surfaces A: Physicochemical and Engineering Aspects*, *238*(1-3), 71–81.
- 800 Ravera, F., Loglio, G., & Kovalchuk, V. I. (2010). Interfacial dilational rheology by  
801 oscillating bubble/drop methods. *Current Opinion in Colloid & Interface Science*,  
802 *15*(4), 217–228.
- 803 Schmidt, D. T., & Payens, T. A. J. (1976). Micellar aspects of casein. In *Surface Colloid*  
804 *Science Volume 9* (John Wiley & Sons, Vol. 9, pp. 165 – 229). New York: Matijevic  
805 E.
- 806 Schuck, P., Dolivet, A., & Jeantet, R. (2012). *Analytical methods for food and dairy powders*.  
807 Chichester, West Sussex; Ames, Iowa: Wiley-Blackwell.
- 808 Schuck, P., Piot, M., Méjean, S., Le Graet, Y., Fauquant, J., Brulé, G., & Maubois, J. L.  
809 (1994). Déshydratation par atomisation de phosphocaseinate natif obtenu par  
810 microfiltration sur membrane. *Le Lait*, *74*(5), 375–388.
- 811 Silva, N. N., Piot, M., de Carvalho, A. F., Violleau, F., Fameau, A.-L., & Gaucheron, F.  
812 (2013). pH-induced demineralization of casein micelles modifies their physico-  
813 chemical and foaming properties. *Food Hydrocolloids*, *32*(2), 322–330.
- 814 Silva, N. N., Saint-Jalmes, A., de Carvalho, A. F., & Gaucheron, F. (2014). Development of  
815 casein microgels from cross-linking of casein micelles by genipin. *Langmuir*, *30*(34),  
816 10167–10175.
- 817 Srinivasan, M., Singh, H., & Munro, P. A. (2001). Creaming stability of oil-in-water  
818 emulsions formed with sodium and calcium caseinates. *Journal of Food Science*,  
819 *66*(3), 441–446.

- 820 Trejo, R., Dokland, T., Jurat-Fuentes, J., & Harte, F. (2011). Cryo-transmission electron  
821 tomography of native casein micelles from bovine milk. *Journal of Dairy Science*,  
822 *94*(12), 5770–5775.
- 823 Udabage, P., McKinnon, I. R., & Augustin, M. A. (2001). Effects of mineral salts and calcium  
824 chelating agents on the gelation of renneted skim milk. *Journal of Dairy Science*,  
825 *84*(7), 1569–1575.
- 826 Vujicic, I., deMan, J. M., & Woodrow, I. L. (1968). Interaction of polyphosphates and citrate  
827 with skim milk proteins. *Canadian Institute of Food Technology Journal*, *1*(1), 17–21.
- 828 Walstra, P. (1990). On the stability of casein micelles. *Journal of Dairy Science*, *73*(8), 1965–  
829 1979.
- 830 Xu, Y., Liu, D., Yang, H., Zhang, J., Liu, X., Regenstein, J. M., Zhou, P. (2016). Effect of  
831 calcium sequestration by ion-exchange treatment on the dissociation of casein micelles  
832 in model milk protein concentrates. *Food Hydrocolloids*, *60*, 59–66.
- 833 Ye, A. (2011). Functional properties of milk protein concentrates: emulsifying properties,  
834 adsorption and stability of emulsions. *International Dairy Journal*, *21*(1), 14–20.
- 835

**Table 1. Distribution of mineral salts in the casein aggregate suspensions.** Colloidal concentrations were determined by deducting soluble from total concentrations. The calcium demineralization rates corresponded to the percentage of solubilized calcium compared to total calcium initially present in the suspensions.

	<b>S1<sub>d</sub></b>	<b>S2<sub>d</sub></b>	<b>S3<sub>d</sub></b>	<b>S4<sub>d</sub></b>
<b>Diffusible Ca (mmol kg<sup>-1</sup>)</b>	0.0	0.0	0.0	0.0
<b>Colloidal Ca (mmol kg<sup>-1</sup>)</b>	11.8	10.3	7.5	3.0
<b>Ca demineralization rate (%)</b>	24	35	56	81
<b>Diffusible Pi (mmol kg<sup>-1</sup>)</b>	2.1	2.0	1.8	1.8
<b>Colloidal Pi (mmol kg<sup>-1</sup>)</b>	3.0	2.5	1.2	0.4
<b>Diffusible Na (mmol kg<sup>-1</sup>)</b>	21.5	21.1	21.2	20.6
<b>Colloidal Na (mmol kg<sup>-1</sup>)</b>	2.6	2.9	3.6	5.3
<b>Diffusible Cl (mmol kg<sup>-1</sup>)</b>	8.3	8.4	8.1	8.0
<b>Colloidal Cl (mmol kg<sup>-1</sup>)</b>	0.0	0.0	0.0	0.0

Table 2. Physicochemical properties of the different CA suspensions.

	S1 <sub>d</sub>	S2 <sub>d</sub>	S3 <sub>d</sub>	S4 <sub>d</sub>
Hydration (g of water g <sup>-1</sup> of dried pellet)	3.0 ± 0.1	2.8 ± 0.1	2.6 ± 0.1	2.1 ± 0.1
Non-sedimentable casein (g kg <sup>-1</sup> )	8.0 ± 0.5	10.3 ± 0.5	15.0 ± 0.4	18.0 ± 0.8
Sedimentable protein (g kg <sup>-1</sup> )	12.9 ± 0.1	11.6 ± 0.1	8.3 ± 1.7	2.3 ± 0.3
Zeta potential of casein aggregates (mV)	-23.5 ± 1.2	-24.4 ± 2.0	-21.5 ± 3.7	-21.5 ± 2.4

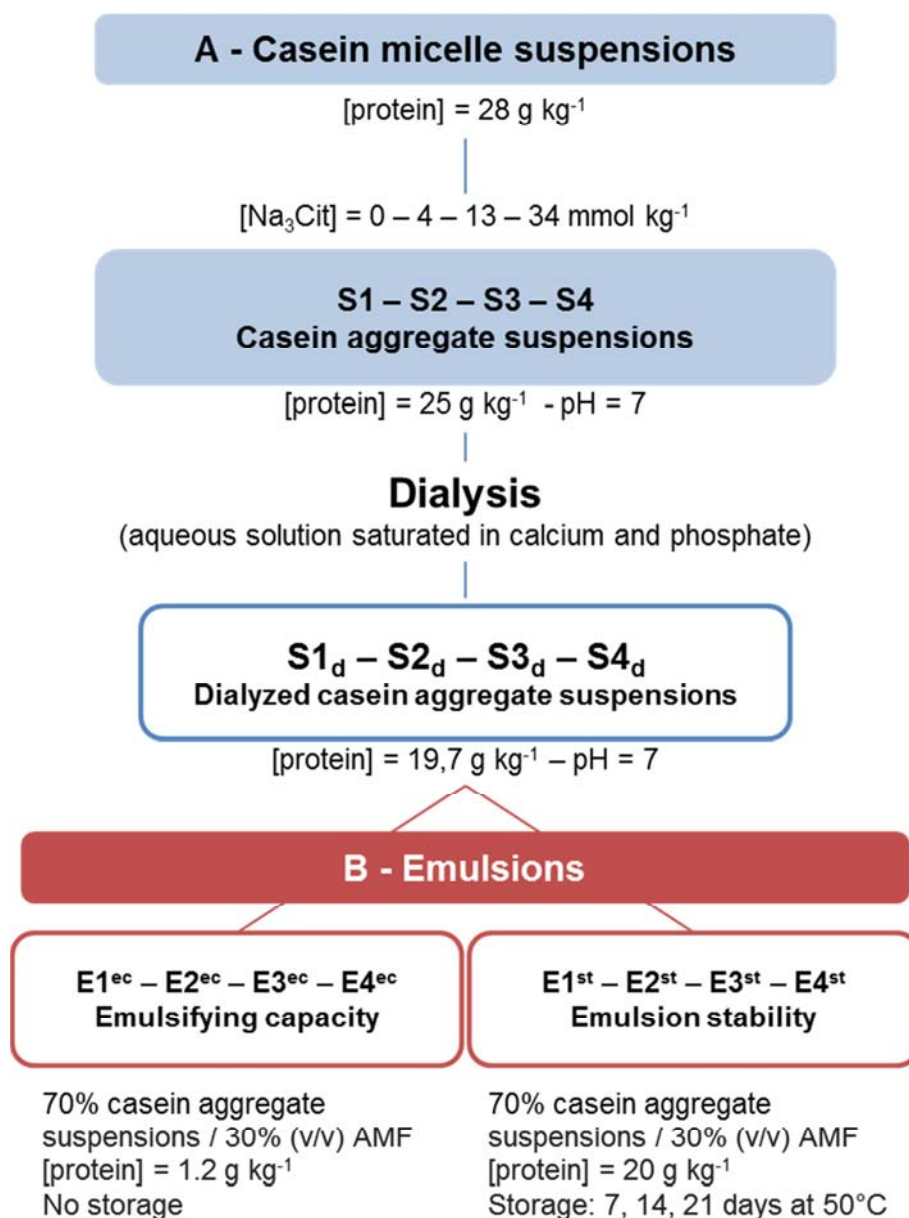


**Fig 1. Preparation of CA suspensions and emulsions.** d, ec and st represent « dialyzed », « emulsifying capacity » and « stability », respectively.



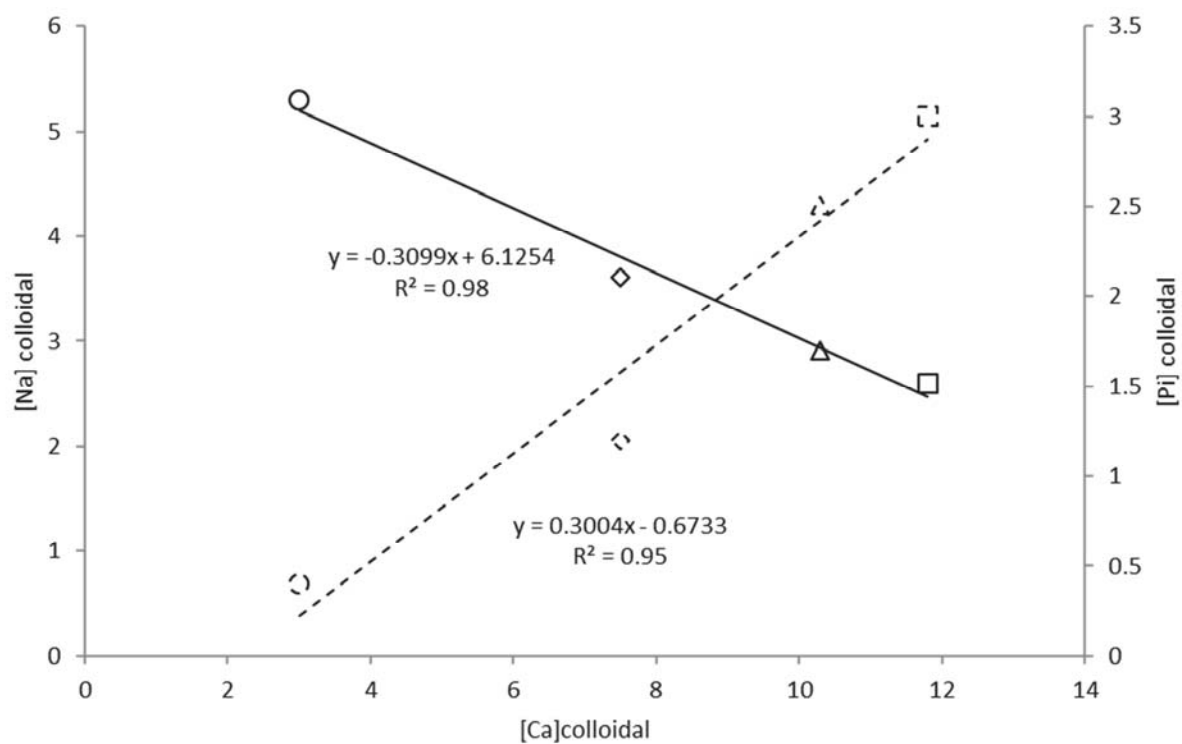


**Fig 2. Correlations between colloidal calcium, sodium and inorganic phosphate concentrations.**

Colloidal inorganic phosphate (—) and colloidal sodium (- - -) as a function of calcium for: S1<sub>d</sub> (o), S2<sub>d</sub> (◊), S3<sub>d</sub> (Δ) and S4<sub>d</sub> (□)

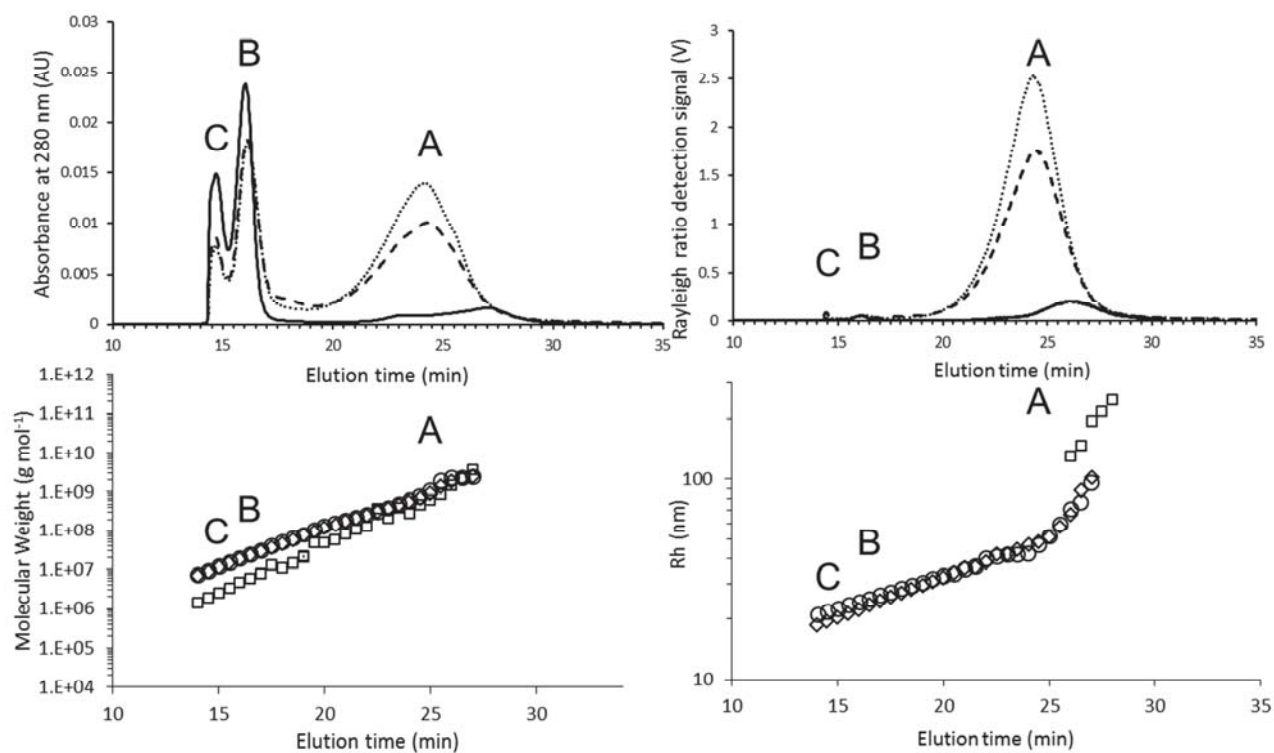


**Fig 3. AsFIFFF determination of structural characteristics of casein aggregates in suspensions.** The UV signal (top left), Rayleigh ratio (top right), molecular mass (bottom left) and hydrodynamic radius (bottom right), were determined for the two extreme suspensions S1<sub>d</sub> (○)(⋯⋯), S4<sub>d</sub> (□)(\_\_\_\_) and one intermediate S2<sub>d</sub> (◇)(- - -) CA suspension as a function of the elution time. Casein micelle-like aggregates (population A), sodium caseinate-like aggregates (population B) and protein monomers (population C) are labeled.

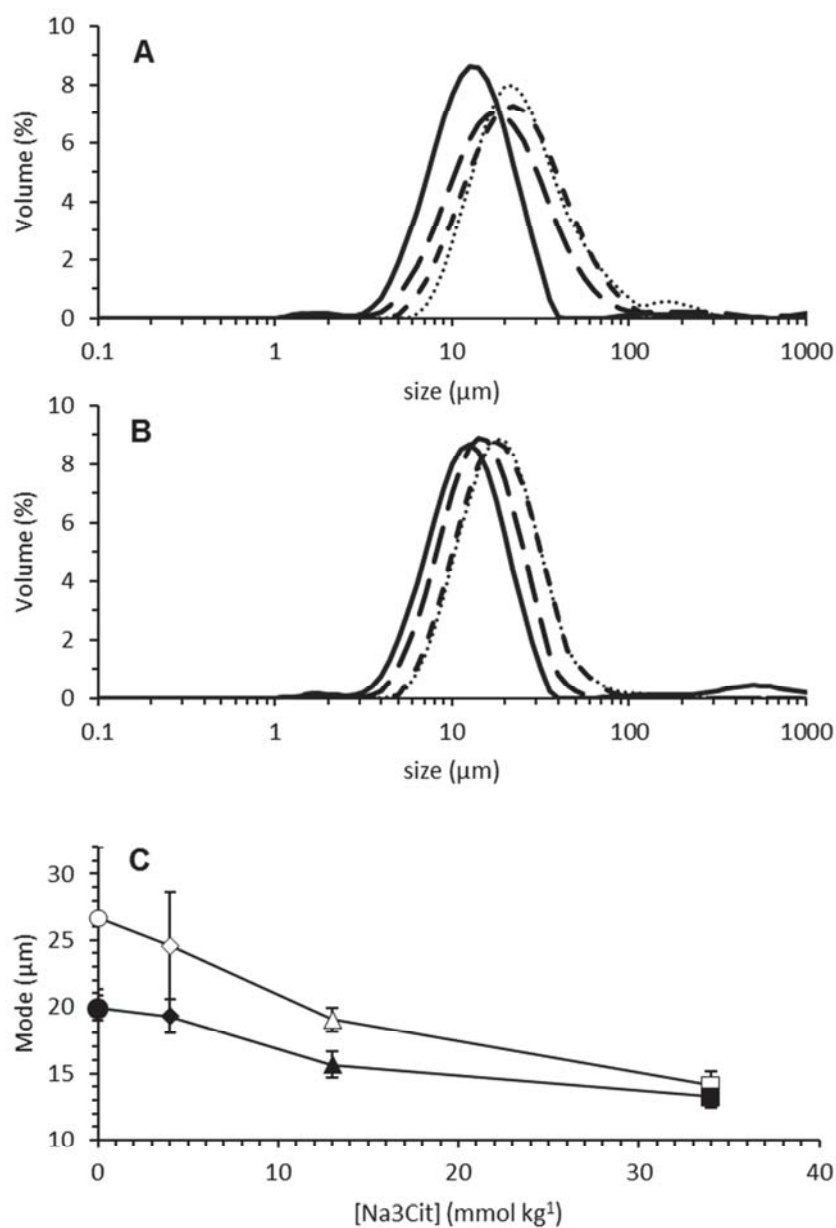


**Fig 4. Size distribution profile of emulsions prepared for the determination of emulsifying capacity ( $E^{ec}$ ).** Emulsions E1<sup>ec</sup> (O)( $\cdots$ ), E2<sup>ec</sup> ( $\diamond$ )( $---$ ), E3<sup>ec</sup> ( $\Delta$ )( $-\ -$ ) and E4<sup>ec</sup> ( $\square$ )( $---$ ) were analyzed as is (A) and diluted ten times in a dissociating medium (aqueous solution of 1% w/w SDS) (B). Evolution of the mode as a function of the concentration of added TSC are represented (C) either in the absence (empty symbols) or presence (filled symbols) of SDS.

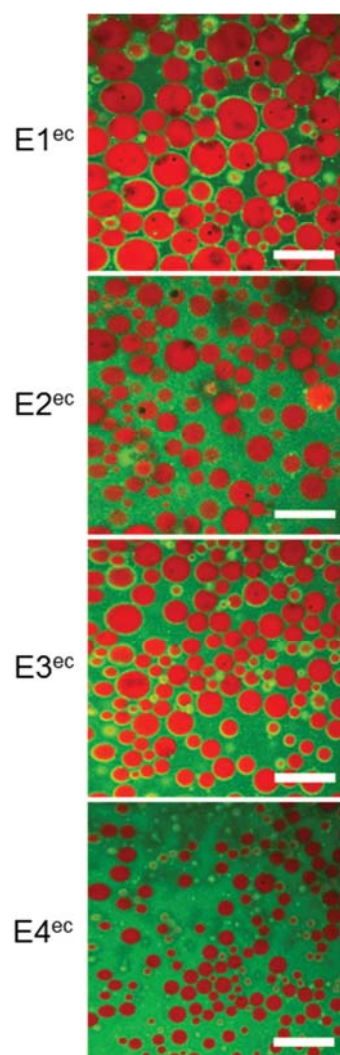


**Fig 5. Confocal laser scanning microscopy images of the emulsions prepared for determination of emulsifying capacity ( $E^{ec}$ ).** Microscopic images were recorded at 50°C using a thermal plate warmer. Milkfat emulsion droplets (in red) surrounded by casein (in green). Scale bars measure 50 μm.

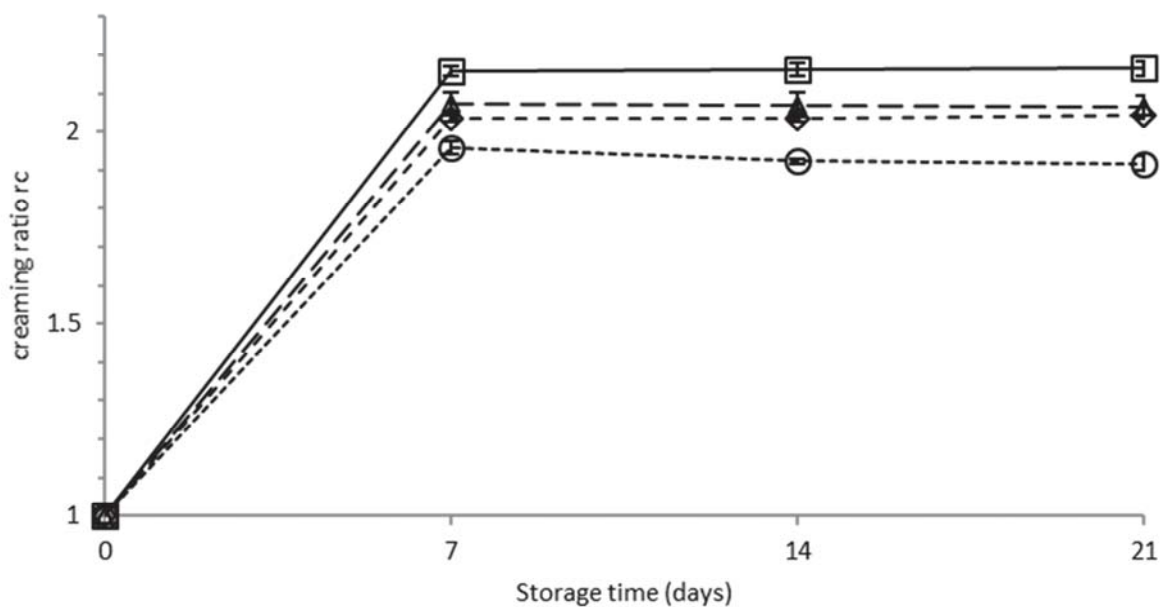


**Fig 6. Time evolution of creaming ratios  $r_c$  of emulsions prepared for the determination of emulsion stability ( $E^{st}$ ).** Creaming ratio defined as  $r_c = H/h$  where  $H$  is the total height of the emulsion and  $h$  the thickness of the creamed layer. Standard deviation bars are represented behind the point marks.

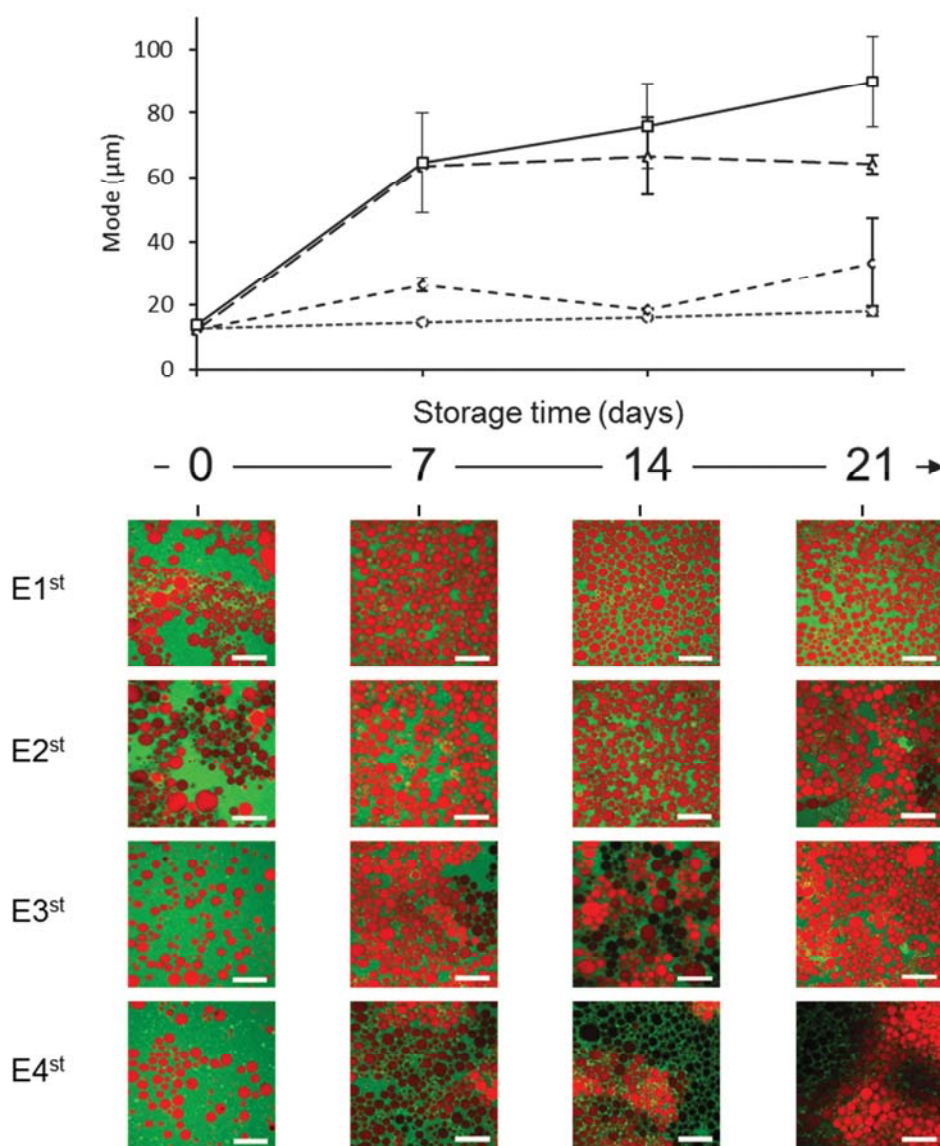


**Fig 7. Microscopic evolution of the emulsions over time ( $E^{st}$ ).** Droplet size (mode) and confocal micrograph evolution as a function of storage time: E1<sup>st</sup> (○)(⋯⋯), E2<sup>st</sup> (◇)(- - -), E3<sup>st</sup> (Δ)(— —) and E4<sup>st</sup> (□)(\_\_\_\_\_). Microscopy images were recorded at 50°C using a thermal plate warmer. Milkfat emulsion droplets (in red) are surrounded by casein (in green). Contrast differences are attributed to the appearance of 3D milkfat droplet flocs in the emulsion that coexisted on different focal planes of the micrographs.

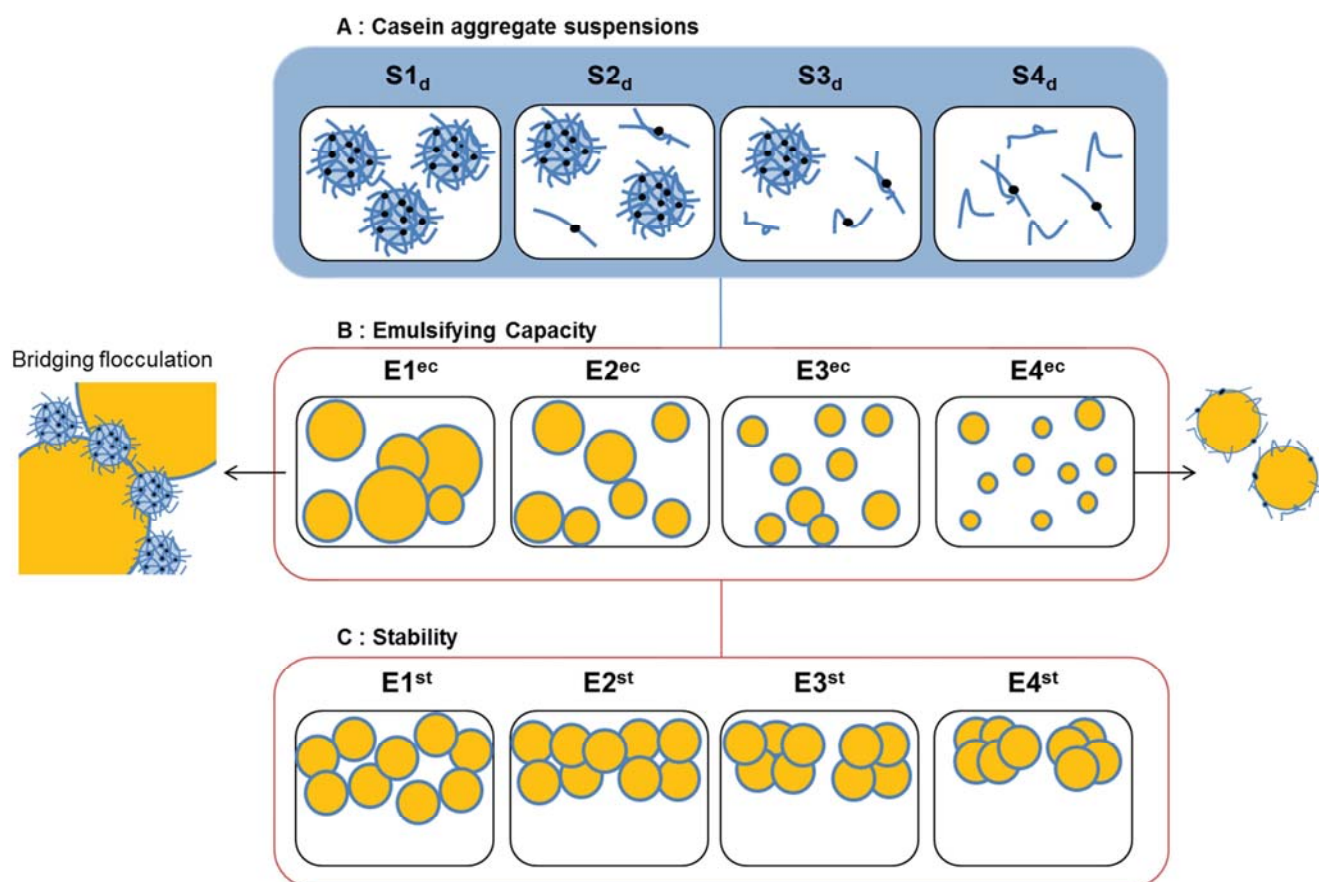


Fig 8. Diagrams of the CA suspensions (A), the emulsions prepared for determination of the emulsifying capacity (B) and the stabilizing capacity (C) of the casein aggregates.

**Highlights:**

Purified casein micelles were modified minerally to form various casein aggregates

Disaggregated casein aggregates had better emulsifying capacity

Emulsions were destabilized by flocculation but protected from coalescence

The casein aggregation state did not affect the coalescence stability of emulsions

Disaggregated casein aggregates induced higher levels of flocculation